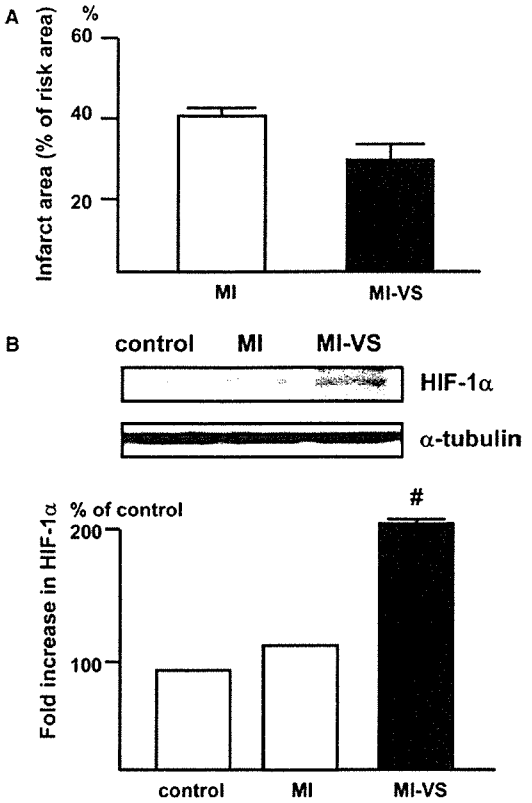

Fig. 6. Vagal nerve stimulation decreases infarcted area with increased HIF-1α expression. (A) A quantitative analysis reveals comparable non-perfused areas in both vagal-stimulated (MI-VS) and non-stimulated (MI) hearts, whereas the infarcted area identified by TTC staining is smaller in the MI-VS heart than in the MI heart. (B) HIF-1α induction in the ischemic heart is increased by vagal stimulation (MI-VS) compared with that in ischemia alone (MI) ($^{\#}P < 0.01$ vs. MI) ($n = 3$).

antiapoptotic activity through various features, such as inhibition of Bad-binding to Bcl-2, caspase 9, Fas and glycogen synthetase kinase-3 [17,18]. These facts imply a definite involvement of Akt activation in cell survival. As shown using dn HIF-1α, ACh inhibited hypoxia-induced cell death through HIF-1α induction via Akt phosphorylation. These results indicate that ACh actually protects cardiomyocytes from hypoxia at the cellular level.

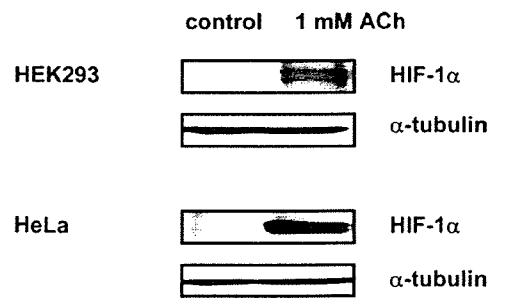

Fig. 7. HIF-1α is induced by ACh under normoxia in other cells. ACh (1 mM) increases HIF-1α protein level in HEK293 and HeLa cells ($n = 3$ each) under normoxia.

4.3. Additional induction of HIF-1α by ACh and vagal stimulation

HIF-1α regulates the transcriptional activities of very diverse genes involved in cell survival and is itself regulated at the posttranslational level by VHL [4,6,7]. Recent studies have shown that HIF-1α is also regulated through a non-hypoxic pathway involving angiotensin II, TNF-α and NO [8,9,19,20]. Therefore, it is speculated that cardiomyocytes possess a similar system for regulating HIF-1α through ACh, independent of the oxygen concentration. Induction of HIF-1α is a powerful cellular response against hypoxia, and further increases in its expression by other pathways may be beneficial. The present results indicate that the significance of ACh or vagal nerve stimulation in hypoxic stress can be attributed to additional HIF-1α induction through dual induction pathways, i.e., hypoxic and non-hypoxic pathways.

The present study has revealed that ACh-mediated HIF-1α induction is widely conserved in other cells. Consistent with a previous report [10], the current results suggest that NO is produced by ACh. According to a report that NO attenuates the interaction between pVHL and HIF-1α through inhibiting PHD activity [21], it is possible that ACh may increase the HIF-1α protein level through NO. Recent studies conducted by Krieg et al. [3] and Xi et al. [22], have provided supportive data compatible with our results, while another study by Hirota et al. [23] also revealed a non-hypoxic pathway for HIF-1α induction by ACh in a human kidney-derived cell line.

The signaling pathway of the muscarinic receptor has been studied extensively, and many pathways are involved in its specific biological effects. Therefore, possible involvement of other pathways in the non-hypoxic induction of HIF-1α cannot be excluded. However, it was demonstrated that dn Akt and dn HIF-1α decreased the effect of ACh. Consistent with a recent study [24], we have revealed that ACh or vagal stimulation protects cardiomyocytes in the acute phase. This observation suggests that the protective effect in the acute phase may result in inhibition of cardiac remodeling in the chronic phase, since vagal stimulation produces additional HIF-1α induction through a non-hypoxic pathway, which increases cell survival.

Acknowledgment: This study was supported by a Health and Labor Sciences Research Grant (H15-PHYSI-001) for Advanced Medical Technology from the Ministry of Health, Labor, and Welfare of Japan.

References

[1] Julian, D.G., Camm, A.J., Frangin, G., Janse, M.J., Munoz, A., Schwartz, P.J. and Simon, P. (1997) Randomised trial of effect of amiodarone on mortality in patients with left-ventricular dysfunction after recent myocardial infarction: EMIAT. European Myocardial Infarct Amiodarone Trial Investigators. Lancet 349, 667–674.

[2] Li, M., Zheng, C., Sato, T., Kawada, T., Sugimachi, M. and Sunagawa, K. (2004) Vagal nerve stimulation markedly improves long-term survival after chronic heart failure in rats. Circulation 109, 120–124.

[3] Krieg, T., Qin, Q., Philipp, S., Alexeyev, M.F., Cohen, M.V. and Downey, J.M. (2004) Acetylcholine and bradykinin trigger preconditioning in the heart through pathway that includes Akt and NOS. Am. J. Physiol. Heart Circ. Physiol. 287, H2606–H2611.

[4] Semenza, G.L. (2003) HIF-1, O(2), and the 3 PHDs: how animal cells signal hypoxia to the nucleus. Cell 107, 1–3.
[5] Kakinuma, Y., Miyauchi, T., Yuki, K., Murakoshi, N., Goto, K. and Yamaguchi, I. (2001) Novel molecular mechanism of increased myocardial endothelin-1 expression in the failing heart involving the transcriptional factor hypoxia-inducible factor-1α induced for impaired myocardial energy metabolism. Circulation 103, 2387–2394.
[6] Maxwell, P.H., Wiesener, M.S., Chang, G.W., Clifford, S.C., Vaux, E.C., Cockman, M.E., Wykoff, C.C., Pugh, C.W., Maher, E.R. and Ratcliffe, P.J. (1999) The tumour suppressor protein VHL targets hypoxia-inducible factors for oxygen-dependent proteolysis. Nature 399, 271–275.
[7] Min, J.H., Yang, H., Ivan, M., Gertler, F., Kaelin Jr, W.G. and Pavletich, N.P. (2002) Structure of an HIF-1alpha-pVHL complex: hydroxyproline recognition in signaling. Science 296, 1886–1889.
[8] Page, E.L., Robitaille, G.A., Pouyssegur, J. and Richard, D.E. (2002) Induction of hypoxia-inducible factor-1alpha by transcriptional and translational mechanisms. J. Biol. Chem. 277, 48403–48409.
[9] Richard, D.E., Berra, E. and Pouyssegur, J. (2000) Non-hypoxic pathway mediates the induction of hypoxia-inducible factor 1alpha in vascular smooth muscle cells. J. Biol. Chem. 275, 26765–26771.
[10] Zanella, B., Calonghi, N., Pagnotta, E., Masotti, L. and Guarnieri, C. (2002) Mitochondrial nitric oxide localization in H9c2 cells revealed by confocal microscopy. Biochem. Biophys. Res. Commun. 290, 1010–1014.
[11] Okudela, K., Hayashi, H., Ito, T., Yazawa, T., Suzuki, T., Nakane, Y., Sato, H., Ishi, H., KeQin, X., Masuda, A., Takahashi, T. and Kitamura, H. (2004) K-ras gene mutation enhances motility of immortalized airway cells and lung adenocarcinoma cells via Akt activation: possible contribution to non-invasive expansion of lung adenocarcinoma. Am. J. Pathol. 164, 91–100.
[12] Chen, J., Zhao, S., Nakada, K., Kuge, Y., Tamaki, N., Okada, F., Wang, J., Shindo, M., Higashino, F., Takeda, K., Asaka, M., Katoh, H., Sugiyama, T., Hosokawa, M. and Kobayashi, M. (2004) Dominant-negative hypoxia-inducible factor-1 alpha reduces tumorigenicity of pancreatic cancer cells through the suppression of glucose metabolism. Am. J. Pathol. 162, 1283–1291.
[13] Du, X.J., Dart, A.M., Riemersma, R.A. and Oliver, M.F. (1990) Failure of the cholinergic modulation of norepinephrine release during acute myocardial ischemia in the rat. Circ. Res. 66, 950–956.
[14] Kim, C.H., Cho, Y.S., Chun, Y.S., Park, J.W. and Kim, M.S. (2002) Early expression of myocardial HIF-1alpha in response to mechanical stresses: regulation by stretch-activated channels and the phosphatidylinositol 3-kinase signaling pathway. Circ. Res. 90, e25–e33.
[15] Sandau, K.B., Zhou, J., Kietzmann, T. and Brune, B. (2001) Regulation of the hypoxia-inducible factor 1alpha by the inflammatory mediators nitric oxide and tumor necrosis factor-alpha in contrast to desferroxamine and phenylarsine oxide. J. Biol. Chem. 276, 39805–39811.
[16] Vanhaesebroeck, B. and Alessi, D.R. (1999) The regulation and activities of the multifunctional serine/threonine kinase Akt/PKB. Exp. Cell Res. 253, 210–229.
[17] Kennedy, S.G., Wagner, A.J., Conzen, S.D., Jordan, J., Bellacosa, A., Tsichlis, P.N. and Hay, N. (1997) The PI3-kinase/Akt signaling pathway delivers an anti-apoptotic signal. Genes Dev. 11, 701–713.
[18] Cross, D.A., Alessi, D.R., Cohen, P., Andjelkovich, M., Hemmings, B.A. and Inhibition of glycogen synthase kinase-3 by insulin mediated by protein kinase, B. (1995) Nature 378, 785–789.
[19] Zhou, J., Schmid, T. and Brune, B. (2003) Tumor necrosis factor-alpha causes accumulation of a ubiquitinated form of hypoxia inducible factor-1alpha through a nuclear factor-kappaB-dependent pathway. Mol. Biol. Cell 14, 2216–2225.
[20] Sandau, K.B., Fandrey, J. and Brune, B. (2001) Accumulation of HIF-1alpha under the influence of nitric oxide. Blood 97, 1009–1015.
[21] Metzen, E., Zhou, J., Jelkmann, W., Fandrey, J. and Brune, B. (2003) Nitric oxide impairs normoxic degradation of HIF-1alpha by inhibition of prolyl hydroxylases. Mol. Biol. Cell 14, 3470–3481.
[22] Xi, L., Taher, M., Yin, C., Salloum, F. and Kukreja, R.C. (2004) Cobalt chloride induces delayed cardiac preconditioning in mice through selective activation of HIF-1{alpha}/AP-1 and iNOS signaling. Am. J. Physiol. Heart. Circ. Physiol. 287, H2369–H2375.
[23] Hirota, K., Fukuda, R., Takabuchi, S., Kizaka-Kondoh, S., Adachi, T., Fukuda, K. and Semenza, G.L. (2004) Induction of hypoxia-inducible factor 1 activity by muscarinic acetylcholine receptor signaling. J. Biol. Chem. 279, 41521–41528.
[24] Wang, H., Yu, M., Ochani, M., Amella, C.A., Tanovic, M., Susarla, S., Li, J.H., Wang, H., Yang, H., Ulloa, L., Al-Abed, Y., Czura, C.J. and Tracey, K.J. (2003) Nicotinic acetylcholine receptor alpha7 subunit is an essential regulator of inflammation. Nature 421, 384–388.

Clinical and Experimental Pharmacology and Physiology (2005) **32**, 911–918

CONTRIBUTION OF BAROREFLEX SENSITIVITY AND VASCULAR REACTIVITY TO VARIABLE HAEMODYNAMIC RESPONSES TO COCAINE IN CONSCIOUS RATS

Michael Traub,* Tamiko Aochi,† Toru Kawada,‡ Toshiaki Shishido,‡ Kenji Sunagawa§ and Mark M Knuepfer

Department of Pharmacological and Physiological Science, St. Louis University School of Medicine, St Louis, Missouri, USA

SUMMARY

1. Baroreflex function is critical for short-term arterial pressure regulation and decreased baroreflex responsivity may predict a predisposition to hypertension and sudden cardiac death. In the present study, we assessed whether baroreflex sensitivity (BRS) and/or vascular reactivity covary with haemodynamic responsiveness to cocaine in vascular and mixed responders.

2. We assessed the heart rate index of BRS in resting animals. We examined dose–response relationships to pressor and depressor agents to determine cardiovascular reactivity. Subsequently, rats were given cocaine (5 mg/kg, i.v.) to classify them as vascular or mixed responders. Vascular responders ($n = 16$) were defined as those rats with a substantial (> 8%) decrease in cardiac output in response to cocaine owing to a larger increase in systemic vascular resistance. The remaining rats ($n = 8$) were mixed responders because they had smaller increases in vascular resistance and little change or an increase in cardiac output.

3. The BRS determined with angiotensin (Ang) II, but not with phenylephrine, was impaired in mixed responders compared with vascular responders. At equipressor doses, there were significantly greater reductions in cardiac output in vascular responders compared with mixed responders in response to phenylephrine or AngII. Methacholine produced greater decreases in heart rate in vascular responders, suggesting greater muscarinic responsivity.

4. We conclude that differences in vascular reactivity to AngII may contribute to differences in haemodynamic response profiles to cocaine in individual rats. More importantly, the differences in vascular responsivity and BRS do not appear to be primary determinants of haemodynamic response variability.

Key words: angiotensin II, cardiac output, cocaine, heart rate index of baroreflex sensitivity, methacholine, nitroprusside, phenylephrine, systemic vascular resistance, vascular responsiveness.

INTRODUCTION

Baroreflex function is important for short-term cardiovascular regulation compensating for transient disturbances in arterial pressure. Increasing arterial pressure to stimulate baroreceptors evokes inhibition of sympathetic activity and enhances parasympathetic activity to minimize the magnitude of the pressor response.[1] Risk analysis studies suggest that decreased heart rate variability, one indicator of diminished baroreflex sensitivity (BRS), is an independent risk factor in humans for the development of arrhythmia[2] and sudden death in patients with congestive heart failure, diabetes mellitus and ischaemic heart disease.[3] Decreased BRS is also common in human subjects with essential hypertension.[4–6] Schwarz *et al.*[7] reported that dogs with coronary occlusion were either prone or resistant to ventricular fibrillation with exercise. Those dogs that were susceptible to fibrillation had reduced BRS, leading the authors to propose that BRS and autonomic imbalance may indicate a predilection to sudden cardiac death. Therefore, reduced BRS has been used to predict a predisposition to the development of cardiovascular disease and sudden cardiac death.

Cocaine evokes different patterns of cardiac output and systemic vascular resistance in rats.[8,9] Although cocaine elicits a pressor response in all rats, some respond with a substantial decrease in cardiac output and a large increase in systemic vascular resistance, whereas others have smaller decreases or an increase in cardiac output and smaller increases in systemic vascular resistance.[8,9] These groups have been designated vascular and mixed responders, respectively.[9] Similar varying haemodynamic response profiles have been observed in response to behavioural stress or amphetamine administration, suggesting that the differences in vascular responses to cocaine are not due to differences in the direct vascular actions of cocaine.[8,10] Because this response may be antagonized by prazosin, pentolinium and adrenal demedullation, the involvement of α-adrenoceptors and activation of the

Correspondence: Dr Mark M Knuepfer, Department of Pharmacological and Physiological Science, St Louis University School of Medicine, 1402 S Grand Blvd, St Louis, MO 63104, USA. Email: knuepfmm@slu.edu

*Present address: Department of Obstetrics and Gynecology, Albert Einstein College of Medicine, Bronx, NY, USA.

†Present address: Arrowhead Regional Medical Center, Colton, CA, USA.

‡Present address: Department of Cardiovascular Dynamics at the National Cardiovascular Research Institute, Osaka, Japan.

§Present address: Department of Cardiovascular Medicine, Graduate School of Medical Sciences, Kyushu University, Fukuoka, Japan.

Received 15 December 2004; revision 3 June 2005; accepted 13 June 2005.

sympathoadrenal system has been implicated.[8,11] Vascular responders have a greater incidence and severity of cocaine-induced ultrastructural myocardial lesions and sudden cardiac death and are more prone to developing hypertension with repeated cocaine or stress.[8,9,12,13] Therefore, we proposed that haemodynamic response patterns to cocaine or behavioural stress may predict the predisposition to develop cardiovascular disease.[9] This may be an important model because clinical observations have suggested that haemodynamic response profiles to behavioural stress in humans vary similarly and those described as vascular responders to acute stress are more prone to develop heart disease and hypertension.[14–18]

Cocaine administration produces varying response patterns in conscious rats due, in part, to muscarinic receptor activation. Pretreatment with atropine methylbromide prevents cocaine-induced decreases in cardiac output and greater increases in systemic vascular resistance in vascular responders, making their haemodynamic responses similar to those in mixed responders.[19,20] Others have reported that cocaine has a direct effect on muscarinic receptors[21,22] or alters catecholamine release from sympathetic nerves.[23,24] Therefore, individual rats may have different haemodynamic response profiles owing to varying responsiveness of peripheral muscarinic receptors to activation by cholinergic agonists.

In the present study, we examined peripheral cardiovascular responsiveness to pressor and depressor agents and differences in the heart rate index of BRS to determine whether these contributed to varying haemodynamic response patterns in vascular and mixed responders. We proposed that vascular responders would have reduced BRS compared with mixed responders similar to humans predisposed to develop cardiovascular disease. We also examined whether vascular reactivity varies between vascular and mixed responders using graded doses of pressor and depressor agents. To produce pressor responses, we used the α-adrenoceptor agonist phenylephrine and the peptide angiotensin (Ang) II. To produce depressor responses, we used the endothelium-dependent muscarinic agonist methacholine and the endothelium-independent agonist nitroprusside. If the differences in haemodynamic responses were due to differences in peripheral vascular responsivity, vascular responders would have greater vasoconstrictor responses to pressor agents. If the differences were dependent on varying muscarinic receptor responsivity, we predicted that the muscarinic agonist, but not nitroprusside, would elicit more profound decreases in cardiac output and heart rate in vascular responders. We discovered that there were differences in BRS between vascular and mixed responders when tested with AngII and that vascular responsiveness to AngII, but not to phenylephrine, is enhanced in vascular responders.

METHODS

Surgical preparation

All experimental protocols were approved by the St Louis University Institutional Animal Care and Use Committee and were in accordance with the *Guide for the Care and Use of Laboratory Animals* (National Research Council, National Academy Press, Washington DC, 1996; http://www.nap.edu/readingroom/books/labrats/). Specific pathogen-free male Sprague-Dawley rats, weighing 285–415 g, were prepared surgically using aseptic techniques under pentobarbital sodium (50 mg/kg, i.p.) anaesthesia. A miniature pulsed Doppler flow probe was placed around the ascending aorta for cardiac output measurement via a midline thoracotomy, as described previously.[8] During recovery (10–14 days), rats were monitored for signs of normal locomotor activity and weight gain and were dosed with cefazolin (10 mg/kg, s.c.) for 1–3 days.

Subsequently, rats were re-anaesthetized with pentobarbital for insertion of sterile cannulas in the left femoral artery and vein for the measurement of arterial pressure and intravenous drug administration, respectively. The cannulas were directed subcutaneously to the posterior neck and sutured in place. Rats were also fitted with leads to measure electrocardiographic data. Multifiber wires (36 awg stainless steel) were implanted in each of the forelimbs, one in the left hind limb and one in the neck (for a ground). All leads were tunnelled subcutaneously to a socket on the skull to record the electrocardiogram. After a recovery period of 2–5 days, during which rats again received cefazolin and were monitored for weight loss, rats were acclimated to a Plexiglas test cage for 6 h. The following day, rats were again acclimated to the test cage for a minimum of 2 h before testing began. If rats displayed continued weight loss (>10% bodyweight) or abnormal ambulation for more than 2 days after either surgery, they were killed with pentobarbital (65 mg/kg, i.p.).

Baroreflex sensitivity determination

Baroreflex sensitivity was determined using phenylephrine, nitroprusside and AngII to raise or lower arterial pressure while measuring the change in heart rate. According to previously reported methods,[4,25,26] we estimated the cardiac index of BRS based on the dynamic response of heart rate to blood pressure alterations, comparing pulse intervals before the change in arterial pressure to a point just before peak arterial pressure change.[26] We avoided the maximum heart rate response because it occurred after the maximum change in arterial pressure and was likely influenced by neurohumoral responses to pressure changes. The slope of the line (heart rate *vs* arterial pressure in b.p.m./mmHg) is the heart rate index of BRS using 10–30 R-R intervals determined electronically. The R-R intervals were excluded if the change in rate between intervals was greater than 50 b.p.m., suggesting an arrhythmia. We attempted to investigate the early changing phase of the baroreflex function curve only by using lower doses of pressor and depressor agents. Therefore, we only studied the steepest part of the relationship. Owing to a lack of data with pressor and depressor responses of greater magnitude (plateau phase), we did not have the appropriate data to fit the logistic equation described by Head and McCarty.[27] The attempt to investigate the entire baroreflex function curve is arguably suspect because the time necessary to reach peak changes in arterial pressure varied between pressor and depressor agents. For example, pressor responses to phenylephrine and AngII occurred relatively quickly (5–7 s), whereas maximum depressor responses to nitroprusside occurred more slowly (10–20 s).

Vascular reactivity protocol

Rats were tested the first day by measuring mean arterial pressure, heart rate and cardiac output responses to a variety of pressor and depressor agents, namely phenylephrine, AngII, nitroprusside and methacholine. Bolus injections of three different doses of each agent were administered as follows: phenylephrine 0.5, 1 and 2 μg/kg; AngII 0.01, 0.05 and 0.1 μg/kg; nitroprusside 2, 3 and 6 μg/kg; methacholine 0.1, 0.5 and 1 μg/kg. Doses were given in alternating pairs, phenylephrine and nitroprusside at progressively larger doses and then AngII and methacholine at progressively larger doses. Each injection was followed by a 0.3 mL saline flush over 20–30 s. Control vehicle (0.9% saline) injections did not produce measurable haemodynamic or behavioural responses. Cardiovascular variables were allowed to return to normal for at least 2 min before administering subsequent doses of vasoactive compounds. To measure vascular reactivity to the drugs, the chart recordings of arterial pressure, heart rate and cardiac output were read before and at the peak change in arterial pressure produced by each drug so that the change in each of the parameters could be measured. From those data, changes in systemic vascular resistance were calculated using Ohm's law.

Cocaine administration

After characterising vascular responsiveness, rats were given cocaine (5 mg/kg, i.v., over 45 s) twice daily (with at least 3 h between dosings) for 2–3 days, as described previously.[8] Briefly, the maximal changes in cardiac output elicited in each trial were averaged in order to classify rats as vascular or mixed responders. Vascular responders were rats with a mean maximal decrease in cardiac output of 8% or more.[8] The remaining rats were classified as mixed responders.

Data acquisition

Ascending aortic blood flow was estimated using a 20 MHz pulsed Doppler flowmeter with a 100 kHz sampling frequency, anti-aliasing and auto-tracking (Department of Bioengineering, University of Iowa, Iowa City, IA, USA). Data were displayed continuously on a chart recorder. Percent changes in systemic vascular resistance and stroke volume were calculated using the mean arterial pressure or heart rate and the ascending aortic blood flow changes (kHz shift). The electrocardiogram (ECG) was recorded using a Grass amplifier (model 7P4) in a Grass Chart Recorder (model 7D; Grass Medical Instruments, Quincy, MA, USA) with a Vetter Data Recorder (model 420; AR Vetter, Rebersburg, PA, USA) to store the recordings before off-line analysis. Data were also displayed and recorded for computer analysis using a 16-channel data acquisition and analysis program (WINDAQ; DATAQ Instruments, Akron, OH, USA) for off-line analysis. The R-R intervals were recorded at 5000 samples/s per channel. Control ECG values were obtained in three separate recording series (each 5 min long) prior to experimentation.

Table 1 Initial baseline cardiovascular parameters

	Mixed responders	Vascular responders	*P*
MAP (mmHg)	114 ± 3 (8)	119 ± 3 (16)	0.3306, $t = 0.99$
HR (b.p.m.)	413 ± 11 (6)	408 ± 6 (16)	0.7057, $t = -0.38$
CO (kHz shift)	9.0 ± 0.8 (8)	10.4 ± 0.6 (16)	0.1565, $t = 1.47$

Data are the mean±SEM with n given in parentheses.
MAP, mean arterial pressure; HR, heart rate; CO, cardiac output.

Data analysis

We evaluated vascular reactivity using two-way analysis of variance (ANOVA). We compared cardiovascular responses in individual rats to three doses of each agonist using a paired approach (within group) and we compared the effects in mixed and vascular responders separately (between group). Post hoc analysis was performed using Bonferroni's (Dunn's) test. Occasional missing data points were interpolated by the software program. Unpaired t-tests with pooled variances were used to compare resting haemodynamic values and both the slope and y-intercepts of the baroreflex function relationship. Linear regression was performed on the heart rate–arterial pressure relationship in each rat in response to phenylephrine, nitroprusside and AngII. All statistical analyses were performed using GB Stat (Dynamic Microsystems, Silver Spring, MD, USA).

RESULTS

Differentiation of cardiovascular responses to cocaine

The resting values for haemodynamic parameters in freely moving, instrumented rats are given in Table 1. There were no significant differences at baseline between vascular and mixed responders. The cardiovascular responses to cocaine (5 mg/kg), as described previously,[8] consisted of a prominent but brief pressor response during the first minute (termed the peak response) and a modest sustained pressor response for several minutes thereafter. For each rat, the cocaine-induced change in cardiac output over the first 60 s for each trial was averaged in order to classify rats as vascular ($n = 16$) and mixed ($n = 8$) responders, as described previously.[8] Vascular responders had a greater reduction in cardiac output than mixed responders (–11.4 ± 1.6 *vs* –1.4 ± 0.5%, respectively; $P < 0.001$, $t = -4.59$) and a greater increase in systemic vascular resistance (46.5 ± 2.9 *vs* 33.1 ± 2.5%, respectively; $P < 0.005$,

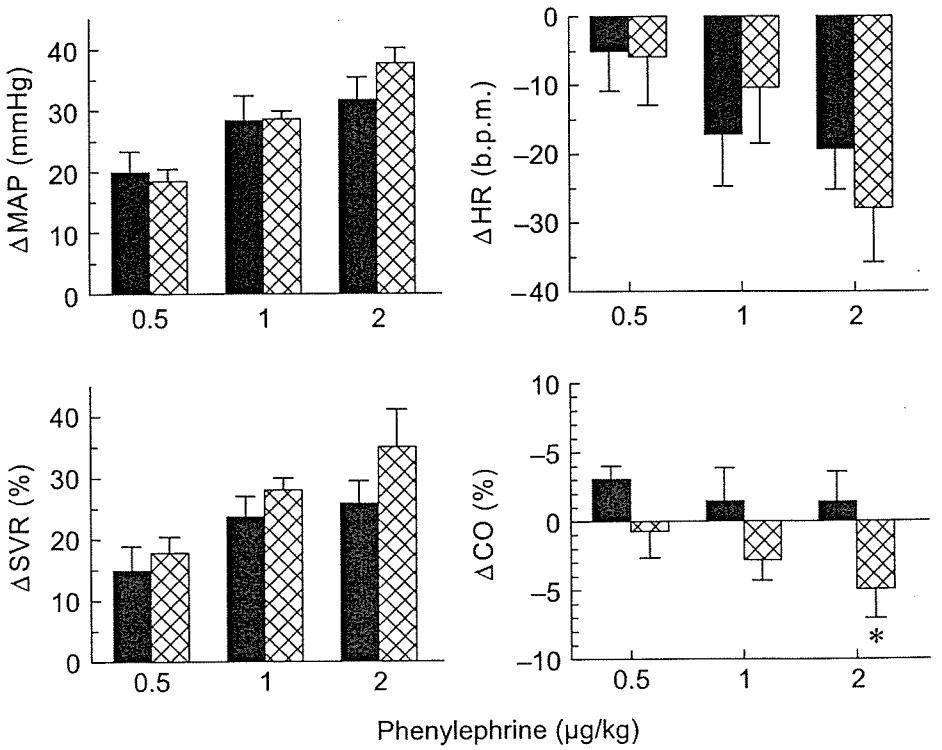

Fig. 1 Cardiovascular responses to graded doses of phenylephrine (0.5, 1 and 2 μg/kg) on mean arterial pressure (MAP), heart rate (HR), cardiac output (CO) and systemic vascular resistance (SVR). Data are the mean±SEM changes in parameters in mixed responders (■) and vascular responders (▨). All responses shown are dose related ($P < 0.0001$, MAP; $P = 0.0062$, HR; $P = 0.0408$, CO; $P = 0.0009$, SVR). Stroke volume was increased slightly but not dose related (data not shown). There was a significant difference in cardiac output responses between vascular and mixed responders ($P = 0.0391$) that was also significant ($P < 0.01$) at the highest dose by post hoc analysis (Bonferroni's test). An asterisk is used to signify significant differences ($P < 0.05$) in vascular responders compared with mixed responders.

$t = 3.11$) after cocaine administration. There were no significant differences in arterial pressure ($P = 0.86$, $t = 0.18$) or heart rate responses ($P = 0.49$, $t = 0.71$) to cocaine during the initial pressor response.

Vascular reactivity to pressor and depressor agents

Before characterising the responses to cocaine in individual rats, differences in vascular reactivity were measured in response to phenylephrine, AngII, nitroprusside and methacholine. Phenylephrine (0.5, 1 and 2 μg/kg, i.v.) elicited brisk pressor responses that were accompanied by a decrease in heart rate (presumably baroreflex mediated) and increases in systemic vascular resistance. In vascular responders, phenylephrine elicited a decrease in cardiac output, whereas it typically produced an increase in mixed responders (Fig. 1). There were no significant differences in the other parameters measured (Table 2). All haemodynamic responses were dose related (Table 2).

Table 2 *F* ratios and significance values for haemodynamic responses

	MAP	HR	CO	SVR
Phenylephrine				
MR versus VR	$F_{1,20} = 0.35$ $P = 0.563$	$F_{1,20} = 0.01$ $P = 0.922$	$F_{1,19} = 4.95$ $P = 0.039$	$F_{1,19} = 1.95$ $P = 0.179$
Dose	$F_{2,42} = 36.1$ $P < 0.0001$	$F_{2,42} = 5.83$ $P = 0.0062$	$F_{2,40} = 3.50$ $P = 0.0408$	$F_{2,40} = 8.57$ $P = 0.0009$
Nitroprusside				
MR versus VR	$F_{1,18} = 0.38$ $P = 0.546$	$F_{1,18} = 3.31$ $P = 0.086$	$F_{1,15} = 0.61$ $P = 0.447$	$F_{1,15} = 0.70$ $P = 0.417$
Dose	$F_{2,38} = 10.63$ $P = 0.0003$	$F_{2,38} = 1.78$ $P = 0.1828$	$F_{2,32} = 1.00$ $P = 0.38$	$F_{2,32} = 6.27$ $P = 0.0056$
Angiotensin II				
MR versus VR	$F_{1,16} = 0.02$ $P = 0.889$	$F_{1,18} = 3.32$ $P = 0.0863$	$F_{1,16} = 6.85$ $P = 0.0194$	$F_{1,16} = 5.66$ $P = 0.031$
Dose	$F_{2,34} = 103.7$ $P < 0.0001$	$F_{2,38} = 1.79$ $P = 0.1828$	$F_{2,34} = 14.81$ $P < 0.0001$	$F_{2,34} = 22.96$ $P < 0.0001$
Methacholine				
MR versus VR	$F_{1,17} = 0.96$ $P = 0.342$	$F_{1,17} = 7.34$ $P = 0.0155$	$F_{1,16} = 2.72$ $P = 0.1197$	$F_{1,16} = 0.85$ $P = 0.3702$
Dose	$F_{2,38} = 21.56$ $P < 0.0001$	$F_{2,36} = 2.13$ $P = 0.1353$	$F_{2,34} = 2.70$ $P = 0.0834$	$F_{2,34} = 17.23$ $P < 0.0001$

MR, mixed responder; VR, vascular responder; MAP, mean arterial pressure; HR, heart rate; CO, cardiac output; SVR, systemic vascular resistance.

Angiotensin II (0.01, 0.05 and 0.1 μg/kg, i.v.) also evoked an increase in arterial pressure in all rats that was dose related and due, primarily, to dose-dependent increases in systemic vascular resistance with concomitant decreases in heart rate. Vascular responders had greater dose-dependent increases in systemic vascular resistance and dose-dependent decreases in cardiac output compared with mixed responders (Fig. 2; Table 2).

Nitroprusside (2, 3 and 6 μg/kg, i.v.) elicited dose-related reductions in arterial pressure due to a decrease in systemic vascular resistance. There were small increases in heart rate and cardiac output that were not dose related. There were no differences between responses in vascular or mixed responders (Fig. 3, Table 2).

The muscarinic agonist methacholine was used to compare muscarinic receptor sensitivity in vascular and mixed responders. Methacholine (0.1, 0.5 and 1 μg/kg, i.v.) elicited dose-related depressor responses due to decreases in systemic vascular resistance. Vascular responders had greater increases in heart rate compared with mixed responders (Fig. 4; Table 2). No other differences in responsivity were observed.

Baroreflex sensitivity

A linear regression of the heart rate versus arterial pressure pulse determined at each R-R interval was used to estimate BRS (Fig. 5). Angiotensin II elicited a decreased slope and *y*-intercept of the BRS

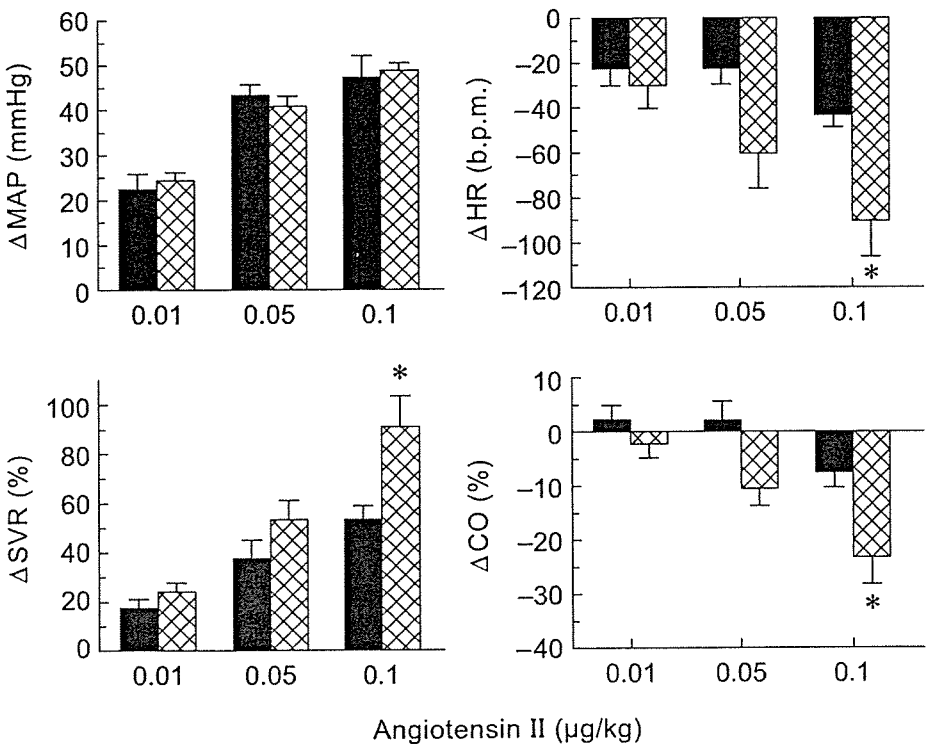

Fig. 2 Angiotensin II (0.01, 0.05 and 0.1 μg/kg, i.v.) elicited dose-related increases in mean arterial pressure (MAP; $P = 0.0003$) and systemic vascular resistance (SVR; $P = 0.0056$). Angiotensin also evoked dose-related reductions in heart rate (HR; $P = 0.0003$) and cardiac output (CO; $P < 0.0001$). The increase in systemic vascular resistance and the decrease in cardiac output were significantly greater in vascular responders (▨) compared with mixed responders (■), with $P = 0.031$ and $P = 0.0194$, respectively. The differences in HR ($P < 0.01$), SVR ($P < 0.05$) and CO ($P = 0.05$) were significant at the highest dose used, as indicated by asterisks.

relationship in mixed responders compared with vascular responders (Table 3). The BRS was not significantly altered in mixed responders in response to phenylephrine and nitroprusside compared with the BRS in vascular responders (Table 3).

DISCUSSION

In the present study, we did not observe differences in the heart rate index of BRS to an α-adrenoceptor agonist or to a direct vasodilator, but did see differences in BRS with AngII administration. There were also differences between vascular and mixed responders in vascular responsivity to AngII and in cardiac responsiveness to AngII, phenylephrine and methacholine administration. The differences in BRS and vascular responsiveness do not seem to be the primary cause of response variability in these animals, but suggest a possible contribution of angiotensin in response variability.

Angiotensin II administration alone produced greater reductions in cardiac output in vascular responders compared with mixed responders similar to the haemodynamic responses we recorded to

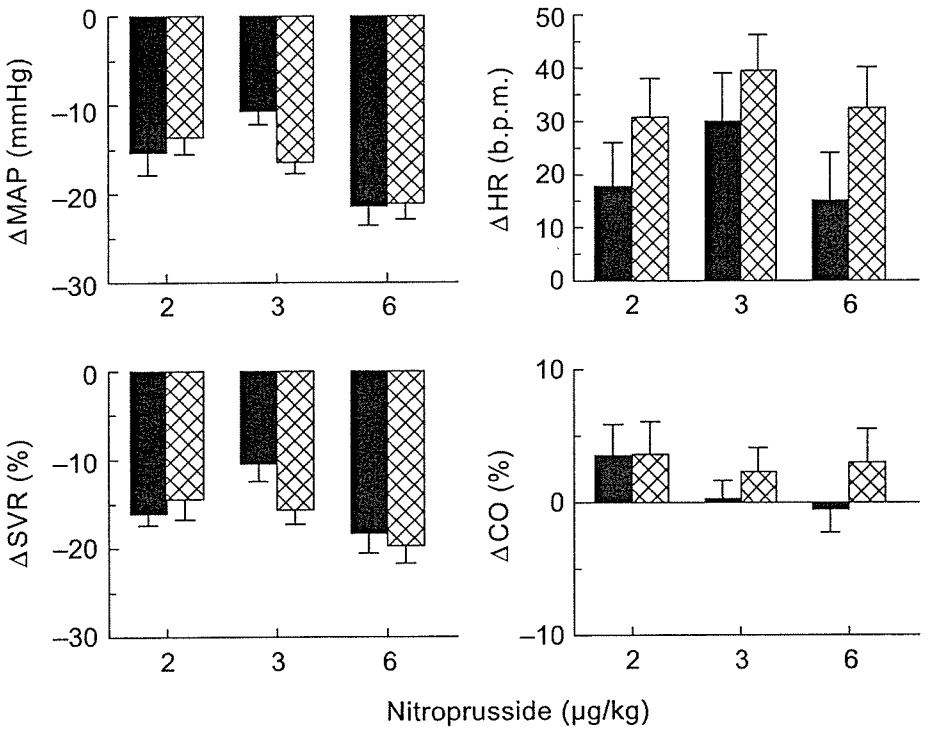

Fig. 3 The effects of nitroprusside (2, 3 and 6 μg/kg, i.v.) on haemodynamic responses in vascular responders (▨) and mixed responders (■). Nitroprusside elicited dose-related reductions in mean arterial pressure (MAP; $P = 0.0003$) due to dose-dependent decreases in systemic vascular resistance (SVR; $P = 0.0056$). There were no differences between vascular and mixed responders. HR, heart rate; CO, cardiac output.

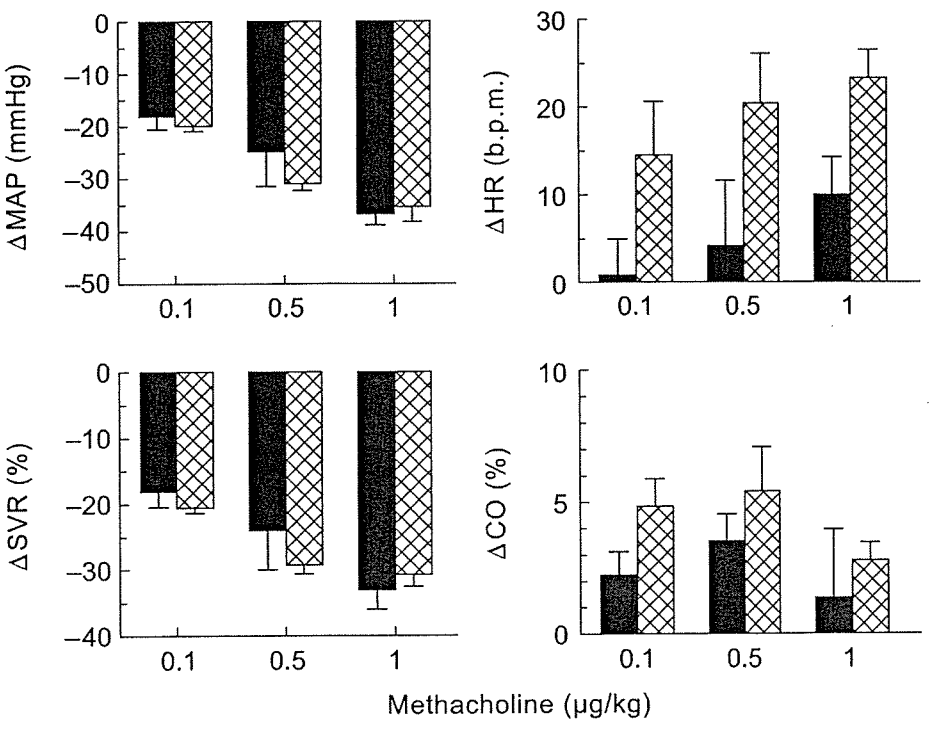

Fig. 4 Methacholine administration (0.1, 0.5 and 1 mg/kg, i.v.) evoked dose-related reductions in mean arterial pressure (MAP; $P < 0.0001$) due to dose-dependent falls in systemic vascular resistance (SVR; $P < 0.0001$). There was a significantly greater increase in heart rate (HR) in vascular responders (▨) compared with mixed responders ($P = 0.0155$; ■). CO, cardiac output.

cocaine (Fig. 1). In addition, we have reported that other psychoactive agents, such as amphetamine or ethanol, elicit a pressor response associated with greater decreases in cardiac output in vascular responders to cocaine.[8,9,28] This apparent anomaly is explained if greater increases in systemic vascular resistance occur in vascular responders in response to these diverse pharmacological stimuli. More importantly, we have noted that vascular responders to cocaine have more negative cardiac output responses and greater increases in systemic vascular resistance to conditional or unconditional behavioural stress.[10] Because it is unlikely that AngII elicits arousal or stress, these findings suggest a role for angiotensin in the mediation of these varying responses.

Angiotensin II elicits a pressor response due to direct vasoconstriction[29,30] and increases noradrenaline release from sympathetic nerve terminals by actions in the ganglia and neuroeffector sites.[31–34] Dendorfer *et al.*[31] reported that intravenous administration of AngII as a bolus resulted in a rapid increase in arterial pressure, sympathetic nerve activity and plasma noradrenaline levels in pithed or ganglionic-blocked rats. Therefore, angiotensin elicits several acute responses to raise arterial pressure after bolus administration. Angiotensin II also elicits central sympathoexcitation due to actions on AT_1 receptors in the circumventricular organs, but this is likely to be a delayed effect and typically overcome by baroreflexes.[35,36] These data demonstrate that AngII has many actions that enhance sympathoexcitation centrally and peripherally. Our data suggest that the relative sensitivity to AngII may vary in vascular and mixed responders. Preliminary evidence from our laboratory suggests that angiotensin may be acting in the central nervous system (CNS).[37,38]

Angiotensin II suppresses baroreflex function by effects both in the CNS and in the carotid sinus.[39–41] Administration of angiotensin-converting enzyme inhibitors has been shown to increase BRS independently of pressure alterations, suggesting a CNS effect.[41,42] Others have suggested that systemic AngII inhibits baroreflex function by local vasoconstriction near nerve endings in the aortic arch of rats and rabbits.[43] Baroreflex function is depressed in response to AngII injected into area postrema or nucleus tractus solitarius.[39,40] Therefore, angiotensin plays a role in modulating BRS. Our data suggest that vascular responders may be less sensitive to this effect compared with mixed responders.

Others have reported that reduced BRS occurs in animals and humans that are prone to the development of hypertension or sudden cardiac death,[6,7] yet the heart rate index of BRS appears to be reduced in the population of rats that are less prone to develop cocaine- or stress-induced elevations in arterial pressure.[8,9,44] This may not, in fact, represent a lower BRS in mixed responders, but could reflect a greater sensitivity to AngII compared with vascular responders. In either case, this appears to be an exception to data described in humans and in dogs with coronary ischaemia.[6,7]

Table 3 Baroreflex responsivity

	Mixed Responders	Vascular Responders	*P*
Phenylephrine relationship			
Slope (b.p.m./mmHg)	−0.9826 ± 0.1828	−1.1245 ± 0.1324	0.2683, $t = 1.16$
Intercept (b.p.m.)	561 ± 26.8	571.0 ± 23.1	0.7758, $t = -0.29$
Nitroprusside relationship			
Slope (b.p.m./mmHg)	−1.2867 ± 0.2367	−1.6202 ± 0.1695	0.2532, $t = 1.19$
Intercept (b.p.m.)	595 ± 29.4	628 ± 17.7	0.3005, $t = -1.08$
Angiotensin II relationship			
Slope (b.p.m./mmHg)	−0.7969 ± 0.1411	−1.6288 ± 0.2714	0.0327,* $t = 2.44$
Intercept (b.p.m.)	520 ± 19.8	610 ± 28.6	0.0331,* $t = -2.44$

Data are the mean±SEM.

Asterisks indicate significant differences ($P < 0.05$) as determined by unpaired Students *t*-test using pooled variances. Only baroreflex plots with $r > 0.40$ were included. Negative values reflect inverse relationships between changes in heart rate and pressure.

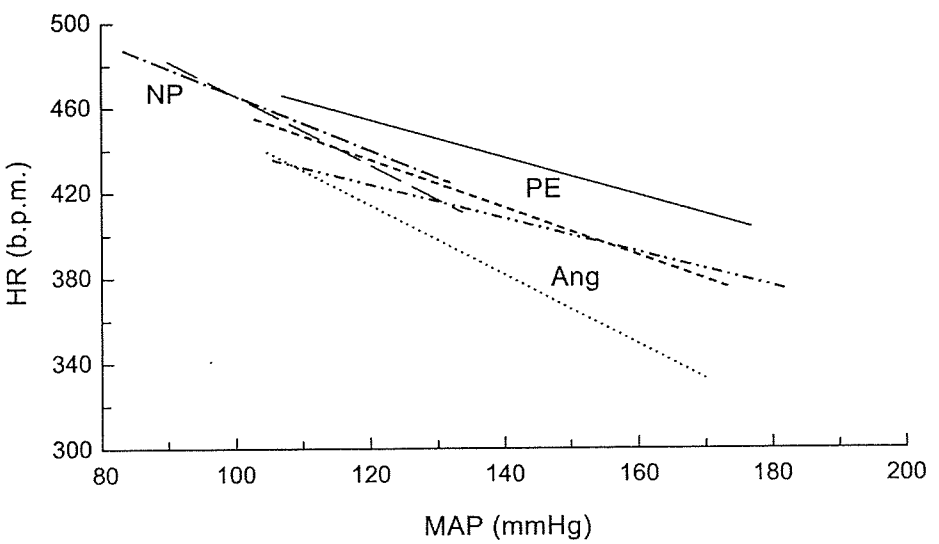

Fig. 5 Linear regression of baroreflex sensitivity in vascular and mixed responders (VR and MR, respectively) in response to bolus doses of nitroprusside (NP), phenylephrine (PE) and angiotensin (Ang) II. (——), MR-PE; (- - - -), VR-PE; (—·—·—), MR-NP; (– – –), VR-NP; (—··—··—), MR-AngII; (·····), VR-AngII. Statistical comparison of linear regressions is described in Table 3.

Stress activates the renin–angiotensin system in addition to the sympathoexcitatory response.[45] Because many of the haemodynamic and neuroendocrine responses to stress are similar to those of cocaine,[9,10] it is possible that the varying effects of angiotensin in these two groups represents a mechanism by which they have varying responses to cocaine and to acute behavioural stress. Alternatively, there may be an arousal or stress component to the administration of angiotensin intravenously. Cocaine has been shown to suppress the baroreflex control of heart rate.[46,47] We argued that this may be due to the actions of the psychostimulant[46] because behavioural stress or arousal suppress baroreflex function.[25,48] We and others have not reported behavioural arousal when angiotensin was administered. Therefore, it is unlikely that there is an arousal or stress component to the drug administration that is different from responses to intravenous administration of phenylephrine or saline. The suppression of baroreflex function by cocaine may also be due to the blockade of noradrenaline reuptake. Kawada *et al.* demonstrated that desipramine reduced the buffering ability of the baroreflex by inhibiting the natural frequency of the transfer function of sympathetic nerve activity to arterial pressure and heart rate responses.[49]

Phenylephrine elicited a greater decrease in cardiac output in vascular responders compared with mixed responders, corroborating an earlier observation.[50] Arterial pressure responses were not different in the present or earlier study. These data again correlate with clinical studies suggesting that differences in α-adrenoceptor activity/responsivity are not responsible for differences in the haemodynamic profile in response to stress in humans.[16]

Methacholine elicited a greater increase in heart rate in vascular responders compared with mixed responders. As a non-selective muscarinic agonist, methacholine elicits vasodilation and slows heart rate. The tachycardia that we recorded suggests that baroreflex-mediated sympathoexcitation overcame the direct effect of methacholine to increase potassium conductance and reduce nodal conduction in the heart. The results could be interpreted as either a greater sympathoexcitatory response in vascular responders or reduced cholinergic receptor sensitivity in cardiac nodal cells of vascular responders. The lack of difference observed with nitroprusside supports the latter conclusion. Moreover, we reported that vascular responders have greater sympathetic responsiveness to cocaine.[50,51] Baroreflex-mediated bradycardia in response to the phenylephrine-induced pressor response has been reported to be primarily dependent on parasympathetic innervation of the heart in conscious rats.[52] We can conclude that the endogenous parasympathetic nervous system does not appear to reflect differences in heart rate responsivity because responses to phenylephrine were not different. In contrast, the exogenous application of a muscarinic agonist does suggest varying sensitivity of cardiac cholinergic receptors.

Cocaine has been reported to act as a competitive inhibitor of M_2 muscarinic cholinergic receptors in the heart and brain.[21,22,53] This has been argued to be irrelevant, except after exposure to high doses, because significant cholinergic binding requires plasma concentrations 20-fold higher than those necessary to produce euphoria.[54] Our laboratory noted that atropine methylbromide reduced the decrease in cardiac output and the increase in systemic vascular resistance elicited by cocaine in vascular responders.[19,20] Muscarinic receptors on adrenergic nerve terminals have been reported to inhibit catecholamine release[23] and, therefore, may reduce cocaine-induced haemodynamic responses by inhibiting the sympathoexcitatory response at the nerve terminal. It has been argued that the pressor response to cocaine may also depend on central cholinergic receptors because intracisternal administration of hemicholinium-3 attenuates the pressor response to intravenous cocaine administration.[55] The present study suggests that there may be differences in the cardiac response to muscarinic agonists, but it is unclear whether the action is mediated centrally or peripherally.

In conclusion, the present studies demonstrate that there is a small but significant difference in the sensitivity of vascular responders to AngII and to methacholine administration. These findings may help explain why responses vary in vascular and mixed responders. If responsiveness to AngII contributes to differences in the haemodynamic response pattern, we should be able to prevent these with central or peripheral administration of angiotensin receptor antagonists. In fact, we have evidence that intracerebroventricular administration of losartan reduced the decrease in cardiac output observed selectively in vascular responders.[37] Indeed, acute cocaine administration has been shown to decrease both plasma renin concentration and activity through a CNS action.[56] Therefore, there is evidence suggesting a role for angiotensin receptors in the varying haemodynamic responsiveness to cocaine in vascular and mixed responders.

ACKNOWLEDGEMENTS

The authors thank Dr Qi Gan for excellent technical assistance in surgically instrumenting these animals. This work was supported by US Public Health Services grants DA05180 and DA13257.

REFERENCES

1. Dampney RAL, Coleman MJ, Fontes MAP *et al.* Central mechanisms underlying short- and long-term regulation of the cardiovascular system. *Clin. Exp. Pharmacol. Physiol.* 2002; **29**: 261–8.
2. Farrell TG, Bahir Y, Cripps T *et al.* Risk stratification for arrhythmic events in postinfarction patients based on heart rate variability, ambulatory electrocardiographic variables and the signal-averaged electrocardiogram. *J. Am. Coll. Cardiol.* 1991; **18**: 687–97.
3. Takase B, Kurita A, Noritake M *et al.* Heart rate variability in patients with diabetes mellitus, ischemic heart disease, and congestive heart failure. *J. Electrocardiol.* 1992; **25**: 79–88.
4. Bristow JD, Honour AJ, Pickering TG *et al.* Diminished baroreflex sensitivity in high blood pressure. *Circulation* 1969; **39**: 48–54.
5. Goldstein DS, Horwitz D, Keiser HR. Comparison of techniques for measuring baroreflex sensitivity in man. *Circulation* 1982; **66**: 432–9.
6. Korner PI, Head GA. Baroreflexes in hypertension. In: Kunos G, Ciriello J (eds). *Central Neural Mechanisms of Blood Pressure Regulation.* Birkhauser, Boston. 1992; 356–74.
7. Schwartz PJ, Vanoli E, Stramba-Badiale M, De Ferrari GM, Billman GE, Foreman RD. Autonomic mechanisms and sudden death: New insights from analysis of baroreceptor reflexes in conscious dogs with and without a myocardial infarction. *Circulation* 1988; **78**: 969–79.
8. Branch CA, Knuepfer MM. Causes of differential cardiovascular sensitivity to cocaine I: Studies in conscious rats. *J. Pharmacol. Exp. Ther.* 1994; **269**: 674–83.
9. Knuepfer MM, Mueller PJ. Review of evidence for a novel model of cocaine-induced cardiovascular toxicity. *Pharmacol. Biochem. Behav.* 1999; **63**: 489–500.
10. Knuepfer MM, Purcell RM, Gan Q, Le KM. Hemodynamic response patterns to acute behavioral stressors resemble those to cocaine. *Am. J. Physiol. Regul. Integr. Comp. Physiol.* 2001; **281**: R1778–86.

11. Knuepfer MM, Gan Q, Mueller PJ. Mechanisms of hemodynamic responses to cocaine in conscious rats. *J. Cardiovasc. Pharmacol.* 1998; **31**: 391–9.
12. Knuepfer MM, Branch CA, Gan Q, Fischer VF. Cocaine-induced myocardial ultrastructural alterations and cardiac output responses in rats. *Exp. Mol. Pathol.* 1993; **59**: 155–68.
13. Williams JB, Keenan SM, Gan Q, Knuepfer MM. Hemodynamic response profile predicts susceptibility to cocaine-induced toxicity. *Eur. J. Pharmacol.* 2003; **464**: 189–96.
14. Brod J. Haemodynamic basis of acute pressor reactions and hypertension. *Br. Heart J.* 1963; **25**: 227–45.
15. Eliot RS. Stress and the heart: Mechanisms, measurement and management. *Postgrad. Med.* 1992; **92**: 237–48.
16. Girdler SS, Hinderliter AL, Light KC. Peripheral adrenergic receptor contributions to cardiovascular reactivity: Influence of race and gender. *J. Psychosom. Res.* 1993; **37**: 177–93.
17. Krantz DS, Manuck SB. Acute psychophysiologic reactivity and risk of cardiovascular disease: A review and methodologic critique. *Psychol. Bull.* 1984; **96**: 435–64.
18. Sherwood A, Hinderliter AL, Light KC. Physiological determinants of hyperreactivity to stress in borderline hypertension. *Hypertension* 1995; **25**: 384–90.
19. Knuepfer MM, Gan Q. Role of cholinergic receptors and cholinesterase activity in hemodynamic responses to cocaine in conscious rats. *Am. J. Physiol.* 1999; **276**: R103–12.
20. Knuepfer MM. Muscarinic cholinergic and β-adrenergic contribution to hindquarters vasodilation and cardiac responses to cocaine. *J. Pharmacol. Exp. Ther.* 2003; **306**: 515–22.
21. Miao L, Qiu Z, Morgan JP. Cholinergic stimulation modulates negative inotropic effect of cocaine on ferret ventricular myocardium. *Am. J. Physiol.* 1996; **270**: H678–84.
22. Sharkey J, Ritz MC, Schenden JA *et al.* Cocaine inhibits muscarinic cholinergic receptors in heart and brain. *J. Pharmacol. Exp. Ther.* 1988; **246**: 1048–52.
23. Lavallée M, de Champlain J, Nadeau RA, Yamaguchi N. Muscarinic inhibition of endogenous myocardial catecholamine liberation in the dog. *Can. J. Physiol. Pharmacol.* 1978; **56**: 642–9.
24. Shannon RP, Stambler BS, Komamura K *et al.* Cholinergic modulation of the coronary vasoconstriction induced by cocaine in conscious dogs. *Circulation* 1993; **87**: 939–49.
25. Brooks D, Fox P, Lopez R, Sleight P. The effect of mental arithmetic on blood pressure variability and baroreflex sensitivity in man. *J. Physiol.* 1978; **280**: P75–6 (Abstract).
26. Smyth HS, Sleight P, Pickering GW. Reflex regulation of arterial pressure during sleep in man: A quantitative method of assessing baroreflex sensitivity. *Circ. Res.* 1969; **24**: 109–21.
27. Head GA, McCarty R. Vagal and sympathetic components of the heart rate range and gain of the baroreceptor–heart rate reflex in conscious rats. *J. Auton. Nerv. Syst.* 1987; **21**: 203–13.
28. Mueller PJ, Gan Q, Knuepfer MM. Ethanol alters hemodynamic responses to cocaine in conscious rats. *Drug Alcohol Depend.* 1997; **48**: 17–24.
29. Peach MJ. Renin–angiotensin system: Biochemistry and mechanisms of action. *Physiol. Rev.* 1977; **57**: 313–70.
30. Timmermans PB, Wong PC, Chiu AT *et al.* Angiotensin II receptors and angiotensin II receptor antagonists. *Pharmacol. Rev.* 1993; **45**: 205–51.
31. Dendorfer A, Thornagel A, Raasch W, Grisk O, Tempel K, Dominiak P. Angiotensin II induces catecholamine release by direct ganglionic excitation. *Hypertension* 2002; **40**: 348–54.
32. Szabo B, Hedler L, Schurr C, Starke K. Peripheral presynaptic facilitatory effect of angiotensin II on noradrenaline release in anesthetized rabbits. *J. Cardiovasc. Pharmacol.* 1990; **15**: 968–75.
33. Aiken JW, Reit E. Stimulation of the cat stellate ganglion by angiotensin. *J. Pharmacol. Exp. Ther.* 1968; **159**: 107–14.
34. Farr WC, Grupp G. Ganglionic stimulation: Mechanism of the positive inotropic and chronotropic effects of angiotensin. *J. Pharmacol. Exp. Ther.* 1971; **177**: 48–55.
35. Sanderford MG, Bishop VS. Angiotensin II acutely attenuates range of arterial baroreflex control of renal sympathetic nerve activity. *Am. J. Physiol. Heart Circ. Physiol.* 2000; **279**: H1804–12.
36. Philips MI. Functions of angiotensin in the central nervous system. *Annu. Rev. Physiol.* 1987; **49**: 413–35.
37. Knuepfer MM, Rowe K, Schwarz JA, Lomax L. Central peptides responsible for the sympathomimetic effects of cocaine. *Regul. Pept.* 2005; **127**: 1–10.
38. Reilly NS, Lomax LL, Knuepfer MM. AT_1 receptors in the median preoptic area (mnPOA) are responsible for regulating hemodynamic responses to cocaine and to behavioral stress. *FASEB J.* 2004; **18**: A675–6 (Abstract).
39. Bishop VS, Sanderford MG. Angiotensin II modulation of the arterial baroreflex: Role of the area postrema. *Clin. Exp. Pharmacol. Physiol.* 2000; **27**: 428–31.
40. Boscan P, Allen AM, Paton JFR. Baroreflex inhibition of cardiac sympathetic outflow is attenuated by angiotensin II in the nucleus of the solitary tract. *Neuroscience* 2001; **103**: 153–60.
41. Heesch CM, Crandall ME, Turbek JA. Converting enzyme inhibitors cause pressure-independent resetting of baroreflex control of sympathetic outflow. *Am. J. Physiol. Regul. Integr. Comp. Physiol.* 1996; **270**: R728–37.
42. Kumagai K, Suzuki H, Ryuzaki M *et al.* Effect of antihypertensive agents on arterial baroreceptor reflexes in conscious rats. *Hypertension* 1992; **20**: 701–9.
43. Munch PA, Longhurst JC. Contrasting effects of vasopressin and angiotensin II on rabbit aortic baroreceptors. *Am. J. Physiol.* 1991; **260**: H811–20.
44. Muller JR, Le KM, Haines WR *et al.* Hemodynamic response pattern predicts susceptibility to stress-induced elevation in arterial pressure in the rat. *Am. J. Physiol. Regul. Integr. Comp. Physiol.* 2001; **281**: R31–7.
45. Aguilera G, Young WS, Kiss A, Bathia A. Direct regulation of hypothalamic corticotropin-releasing hormone neurons by angiotensin II. *Neuroendocrinology* 1995; **61**: 437–44.
46. Knuepfer MM, McCann RK, Kamalu L. Effects of cocaine on baroreflex control of heart rate in conscious rats. *J. Auton. Nerv. Syst.* 1993; **43**: 257–66.
47. Trouvé R, Nahas G, Latour C. Inhibition by cocaine of the baroreflex in the rat. *Proc. Soc. Exp. Biol. Med.* 1992; **201**: 215–18.
48. Schlor KH, Stumpf H, Stock G. Baroreceptor reflex during arousal induced by electrical stimulation of the amygdala or by natural stimuli. *J. Auton. Nerv. Syst.* 1984; **10**: 157–65.
49. Kawada T, Miyamoto T, Uemura K *et al.* Effects of neuronal norepinephrine uptake blockade on baroreflex neural and peripheral arc transfer characteristics. *Am. J. Physiol. Regul. Integr. Comp. Physiol.* 2004; **286**: R1110–20.
50. Branch CA, Knuepfer MM. Causes of differential cardiovascular sensitivity to cocaine II: Sympathetic, metabolic and cardiac effects. *J. Pharmacol. Exp. Ther.* 1994; **271**: 1103–13.
51. Purcell RM, Gan Q, Knuepfer MM. Variable renal sympathetic responses to cocaine in rats. *FASEB J.* 2001; **15**: A801 (Abstract).
52. Stornetta RL, Guyenet PG, McCarty RC. Autonomic nervous system control of heart rate during baroreceptor activation in conscious and anesthetized rats. *J. Auton. Nerv. Syst.* 1987; **20**: 121–7.
53. Flynn DD, Vaishnav AA, Mash DC. Interactions of cocaine with primary and secondary recognition sites on muscarinic receptors. *Mol. Pharmacol.* 1992; **41**: 736–42.
54. Schneider DJ. Cardiac ramifications of cocaine abuse. *Coron. Artery Dis.* 1991; **2**: 267–73.
55. Buccafusco JJ, Davis JA, Shuster LC, Buccafusco CJ, Gattu M. The importance of brainstem cholinergic neurons in the pressor response to cocaine. *J. Pharmacol. Exp. Ther.* 2005; **312**: 179–91.
56. Van de Kar LD, Levy AD, Rittenhouse PA *et al.* Cocaine-induced suppression of renin secretion is mediated in the brain: Investigation of cardiovascular and local anesthetic mechanisms. *Brain Res. Bull.* 1992; **28**: 837–42.

Japanese Journal of Physiology, 55, 157–163, 2005

Dynamic Characteristics of Carotid Sinus Pressure-Nerve Activity Transduction in Rabbits

Toru KAWADA, Kenta YAMAMOTO, Atsunori KAMIYA, Hideto ARIUMI, Daisaku MICHIKAMI, Toshiaki SHISHIDO, Kenji SUNAGAWA*, and Masaru SUGIMACHI

Department of Cardiovascular Dynamics, Advanced Medical Engineering Center, National Cardiovascular Center Research Institute, Osaka, 565-8565 Japan; and *Department of Cardiovascular Medicine, Graduate School of Medical Sciences, Kyushu University, Fukuoka, 812-8582 Japan

Abstract: The dynamic characteristics of the baroreflex neural arc from pressure input to efferent sympathetic nerve activity (SNA) reveal derivative characteristics in the frequency range of 0.01 to 0.8 Hz (i.e., the baroreflex gain augments with increasing frequency) and high-cut characteristics in the frequency range above 0.8 Hz (i.e., the baroreflex gain decreases with increasing frequency) in rabbits. The derivative characteristics accelerate the arterial pressure regulation via the baroreflex. The high-cut characteristics preserve the baroreflex gain against pulsatile pressure by attenuating the high-frequency components less necessary for arterial pressure regulation. However, to what extent the carotid sinus baroreceptor transduction from pressure input to afferent baroreceptor nerve activity (BNA) contributes to these characteristics remains unanswered. To test the hypothesis that the carotid sinus pressure-BNA transduction partly explains the derivative characteristics but not the high-cut characteristics, we examined the dynamic BNA response to pressure input in the frequency range from 0.01 to 3 Hz by using a white noise analysis in 7 anesthetized rabbits. The transfer function from pressure input to BNA showed slight derivative characteristics in the frequency range from 0.01 to 0.3 Hz with approximately a 1.7-fold increase in dynamic gain, but it showed no high-cut characteristics. In conclusion, the carotid sinus baroreceptor transduction partly explained the derivative characteristics but not the high-cut characteristics of the baroreflex neural arc. The present results suggest the importance of the central processing from BNA to efferent SNA to account for the overall dynamic characteristics of the baroreflex neural arc. [The Japanese Journal of Physiology 55: 157–163, 2005]

Key words: systems analysis, transfer function, baroreflex neural arc.

The carotid sinus baroreflex is among the most important negative feedback systems that stabilize arterial pressure (AP) during daily activity. A knowledge of the dynamic characteristics of a given system is important for an in-depth understanding of the system behavior. In previous studies [1–4], we applied a white noise analysis to the carotid sinus baroreflex in rabbits and assessed the transfer function of the baroreflex neural arc from pressure input to efferent sympathetic nerve activity (SNA). The neural arc transfer function revealed two distinct features. One relates to the derivative characteristics in which the baroreflex gain augments with increasing frequency from 0.01 to 0.8 Hz. The derivative characteristics accelerate the dynamic AP regulation by the carotid sinus baroreflex [1]. The other feature relates to the high-cut characteristics in which the baroreflex gain decreases with increasing frequency above 0.8 Hz [4]. The high-cut characteristics prevent the high-frequency components from saturating the baroreflex central processing and preserve the baroreflex gain against pulsatile pressure. However, whether the carotid sinus

Received on Jun 30, 2005; accepted on Jul 29, 2005; released online on Aug 5, 2005; DOI: 10.2170/jjphysiol.R2122
Correspondence should be addressed to: Toru Kawada, Department of Cardiovascular Dynamics, Advanced Medical Engineering Center, National Cardiovascular Center Research Institute, 5-7-1 Fujishirodai, Suita, Osaka, 565-8565 Japan. Phone:+81-6-6833-5012 (Ext. 2427), Fax: +81-6-6835-5403, E-mail: torukawa@res.ncvc.go.jp

baroreceptor transduction from the pressure input to afferent baroreceptor nerve activity (BNA) or the central processing from the afferent BNA to efferent SNA played a major role in forming derivative and high-cut characteristics remains unanswered.

The dynamic characteristics of the pressure input-nerve activity transduction have been examined by the use of step and sinusoidal inputs [5–7]. Although these classical inputs and resulting outputs are easy to interpret, they have a critical drawback because only limited aspects of the system characteristics can be identified. In other words, the system response to untested input signals cannot be predicted precisely because the untested input signals may have frequency components that the step or sinusoidal input does not have. A white noise input, which is rich in frequency components, is most appropriate for a thorough examination of a given system [8–10]. We have identified the dynamic characteristics from pressure input to aortic depressor nerve activity in rabbits with the white noise analysis [11]. The results of that study suggest that the derivative characteristics of the baroreflex neural arc may be partly attributable to the pressure input-nerve activity transduction, whereas the high-cut characteristics may be primarily attributable to the central processing from BNA to efferent SNA. However, regional differences of the transduction properties have been reported between carotid sinus and aortic baroreceptors [12]. Hence the purpose of the present study was to directly estimate dynamic characteristics of the carotid sinus pressure (CSP)-BNA transduction by using the white noise analysis. The results confirmed the hypothesis that the CSP-BNA transduction partly explained the derivative characteristics, but not the high-cut characteristics.

METHODS

Surgical preparations. The animals were cared for in strict accordance with the Guiding Principles for the Care and Use of Animals in the Field of Physiological Sciences approved by the Physiological Society of Japan. Seven Japanese white rabbits weighing 2.7 to 3.1 kg were anesthetized by intravenous injection (2 ml/kg) of a mixture of urethane (250 mg/ml) and α-chloralose (40 mg/ml), and mechanically ventilated with oxygen-enriched room air. A supplemental dose of these anesthetics was administered continuously (0.5 $ml \cdot kg^{-1} \cdot h^{-1}$) to maintain an appropriate level of anesthesia. AP was monitored by a high-fidelity pressure transducer (Millar Instruments, Houston, TX) inserted via the right femoral artery. Following a midline cervical incision, the right external carotid artery was exposed, ligated at two positions, and sectioned in between to access the tissue between the external and internal carotid arteries. A carotid sinus nerve was identified by using a pair of platinum electrodes and by confirming AP-synchronous activity on a loudspeaker. The nerve was then freed from the platinum electrodes during the following carotid sinus isolation procedure. The right internal carotid artery and other small branches arising from the carotid sinus area were ligated. A catheter (0.6 mm internal diameter, 15 cm long) was introduced from the right common carotid artery, and the carotid sinus blind sac was filled with warmed physiological saline. CSP was measured at the end of the catheter opposite the carotid sinus and was controlled by a servo-controlled piston pump (model ET-126A, Labworks, Costa Mesa, CA). A small amount of leakage from the isolated carotid sinus, if any remained, was replenished from the pump during the experiment. After completing the carotid sinus isolation procedure, we attached a pair of stainless steel wire electrodes to the previously identified carotid sinus nerve (Bioflex wire AS633, Cooner Wire, CA) for the multifiber recording of BNA. The nerve and electrodes were secured with silicone glue (Kwik-Cast, World Precision Instruments, Inc.) for insulation. The preamplified nerve signal was band-pass filtered at 150–1,000 Hz. It was then full-wave rectified and low-pass filtered at 30 Hz to quantify the nerve activity. The left carotid sinus nerve, bilateral aortic depressor nerves, and bilateral vagal nerves were all sectioned. The body temperature of the experimental animal was maintained at approximately 38°C with a heating pad.

In three of the seven animals, the controlled CSP was compared with the actual pressure imposed on the carotid sinus area after the BNA recording experiment had finished. After carefully removing the electrodes and silicone glue, we loosened a ligature to the external carotid artery. A catheter-tip pressure transducer (Millar Instruments, Houston, TX) was then introduced into the carotid sinus from the external carotid artery. A signal from the transducer served as the actual pressure imposed on the isolated carotid sinus area.

Protocols. Random input protocol: We randomly changed CSP to either 80 or 120 mmHg with a switching interval of 50 ms for 15 min in order to estimate the dynamic characteristics of the CSP-BNA transduction.

Stepwise input protocol: We increased CSP from 20 to 180 mmHg every minute with a step size of 20

mmHg in order to estimate the static characteristics of the CSP-BNA transduction.

We recorded CSP, BNA and AP at a sampling rate of 200 Hz by using a 12-bit analog-to-digital converter. The data were stored on the hard disk of a dedicated laboratory computer system for later analysis.

Data analysis. In the random input protocol, we estimated the transfer function, $H(f)$, from CSP input to BNA output according to previous studies [1–4, 8, 10–11, 13]. We normalized the transfer function so that the average transfer gain value below 0.02 Hz became unity and expressed BNA in arbitrary units for dynamic analysis (AU_{dyn}). We also calculated the coherence function, $Coh(f)$, between CSP and BNA [1–4, 8, 10–11, 13]. A unity coherence value indicates perfect linear dependence whereas zero coherence value indicates total independence between CSP and BNA.

In the stepwise input protocol, we calculated the steady-state BNA values by averaging the data during the last 10 s of each CSP level. We then scaled these values so that their minimum and maximum BNA values became 0 and 100 arbitrary units (AU_{stat}), respectively, for static analysis. We performed a regression analysis for the four-parameter logistic function using Eq. 1 [14].

$$y = \frac{P_1}{1+\exp[P_2(x-P_3)]} + P_4 \qquad (1)$$

where P_1 is the response range (i.e., the difference between the maximum and minimum values of y), P_2 is the slope coefficient, P_3 is the midpoint on the input axis, and P_4 is the minimum value of y. The fitting error (err%) for the logistic function was evaluated by using Eq. 2.

$$err\% = \frac{\sum_{k=1}^{N}[u(k)-y(k)]^2}{\sum_{k=1}^{N}[u(k)-\bar{u}]^2} \times 100 \qquad (2)$$

where u(k) and y(k) indicate the measured and predicted BNA values at each CSP level. N indicates the number of data points analyzed, and $\bar{u}$ represents the average value of u(k) when k spans from 1 to N.

RESULTS

The dynamic characteristics of the pressure transduction from CSP to actual pressure imposed on the carotid sinus area are depicted in Fig. 1A. The gain plot (top panel) indicates the ratio of actual pressure to CSP in the frequency domain. The controlled CSP faithfully reflected the actual pressure up to 3 Hz. The ratio was greatly dispersed above 3 Hz. The phase plot (middle panel) indicates that the phase delay was negligible up to 1 Hz. The phase delay at 3 Hz was approximately 0.33 radians. The coherence plot (bottom panel) indicates that the coherence was unity up to 3 Hz and decreased slightly above 3 Hz.

Figure 1B shows a typical time series of CSP and BNA obtained from the random input protocol. CSP was changed according to a binary white noise sequence. BNA varied in response to the CSP input. When CSP was increased, BNA was increased, and vice versa.

Figure 1C illustrates the transfer function from CSP to BNA averaged from all animals. The gain plot (top), phase plot (middle) and coherence plot (bottom) are presented. In each plot the thick line indicates the mean value, and the thin lines indicate the mean ± SEM values. In the gain plot, the gain value at the lowest frequency was normalized to unity. The gain increased with increasing frequency from 0.01 to 0.3 Hz and showed a relatively constant value of approximately 1.7 up to 3 Hz. In the phase plot, the phase value led slightly in the frequency range from 0.01 to 0.2 Hz and close to zero radians from 0.2 to 1 Hz. Although the phase delayed above 1 Hz, the delay is most likely attributable to the phase delay between CSP and actual pressure shown in Fig. 1A. In the coherence plot, the coherence was approximately 0.6 at the lowest frequency and increased to 0.8 in the frequency range of 0.1 to 3 Hz.

Figure 2A depicts the typical time series of CSP and BNA obtained from the stepwise input protocol. The CSP and BNA data were resampled at 2 Hz for these panels. An increase in CSP increased BNA in the CSP range of 40 to 160 mmHg. When the BNA response to stepwise input was obvious, it was greater at the onset of pressure change and then decayed to the steady-state value. The steady-state BNA value was not necessarily greater at 40 mmHg than at 20 mmHg across the animals. The steady-state BNA value was not necessarily greater at 180 mmHg than at 160 mmHg.

Figure 2B illustrates the static input-output relationship between CSP and BNA averaged from all animals. The closed circles and error bars represent mean and mean ± SEM values of BNA at each CSP level, respectively. The solid curve indicates the logistic function constructed from the averaged parameters shown in Table 1.

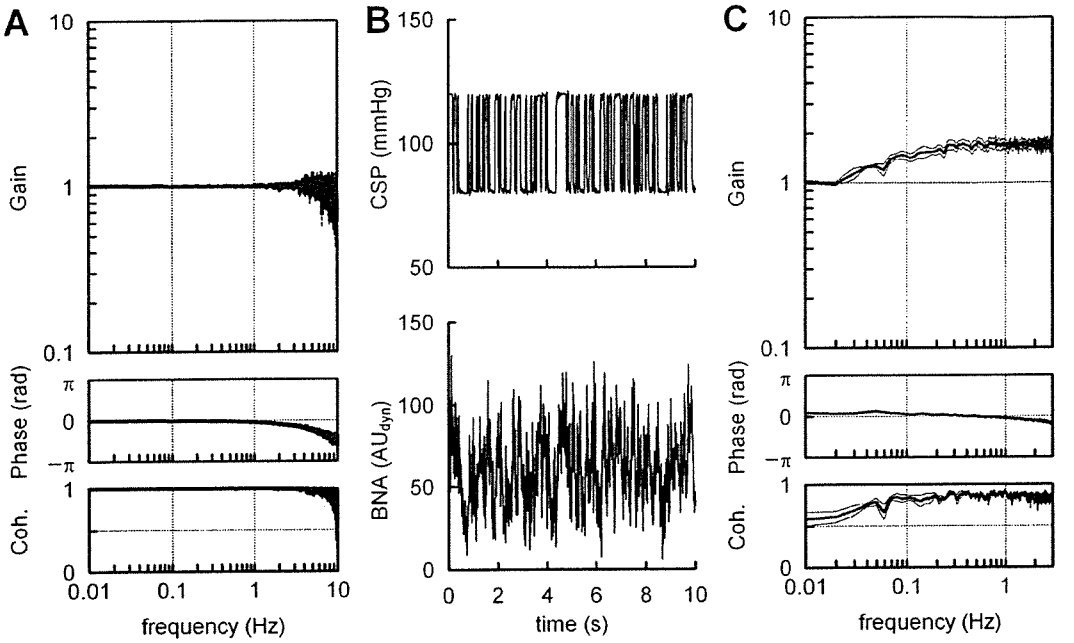

Fig. 1. A: The transfer function from controlled carotid sinus pressure (CSP) to actual pressure imposed on the carotid sinus area. The gain plot represents the ratio of actual pressure to CSP in the frequency domain. The phase plot represents the phase difference between CSP and actual pressure. The coherence (Coh.) shows the extent of linearity between CSP and actual pressure. Based on the transfer function from CSP to actual pressure, we employed the transfer function data up to 3 Hz in the analysis of CSP-nerve activity transduction. The phase difference between CSP and actual pressure in the frequency range between 1 and 3 Hz was taken into account in the interpretation of the CSP-nerve activity transduction. **B: Representative time series of CSP and afferent baroreceptor nerve activity (BNA) during the random input protocol.** CSP was changed according to a binary white noise signal with a switching interval of 50 ms. AU_{dyn}: arbitrary units for dynamic analysis. **C: Transfer function from CSP to BNA averaged from all animals.** The gain plot, phase plot, and coherence are shown. The transfer gain increased with increasing frequency from 0.01 to 0.3 Hz and showed a relatively constant value of approximately 1.7 up to 3 Hz. In all panels, thick and thin lines represent mean and mean ± SEM values.

Table 1 summarizes the parameters of the logistic function fitted to the steady-state CSP-BNA relationship obtained from the stepwise input protocol. The fitting error to the logistic function was less than 1% relative to the total variation in steady-state BNA values.

DISCUSSION

Dynamic characteristics of the carotid sinus baroreceptor transduction. Because of technical difficulty with the in situ preparation, we could not measure actual pressure imposed on the carotid sinus area and record BNA simultaneously. Therefore we measured controlled CSP and actual pressure imposed on the carotid sinus area simultaneously. As shown in Fig. 1A, the controlled CSP faithfully reflected the actual pressure up to 3 Hz. Above this frequency the ratio of actual pressure to CSP became greatly dispersed among animals. Because the compliance of the isolated area would depend on the vascular configuration and inevitably differ among animals, the pressure transduction in the frequencies above 3 Hz may reveal significant inter-individual differences. Actually, the insertion of the catheter-tip micromanometer itself might have affected the compliance of the isolated area to some degree. The phase delay reached approximately 0.33 radians at 3 Hz, which corresponds to 0.018 s of pure dead time. Although this value was not negligible, we employed the transfer function data up to 3 Hz in the analysis of the CSP-BNA relationship because the inter-individual differences in the phase delay were

Table 1. Parameters of the logistic function fitted to the steady-state CSP-BNA relationship.

Response range, P_1, AU_{stat}	98.1 ± 2.4
Slope coefficient, P_2, $mmHg^{-1}$	−0.072 ± 0.010
Midpoint pressure, P_3, mmHg	89.9 ± 3.4
Minimum value, P_4, AU_{stat}	0.05 ± 1.98
err%	0.9 ± 0.5

Data are means±SEM.

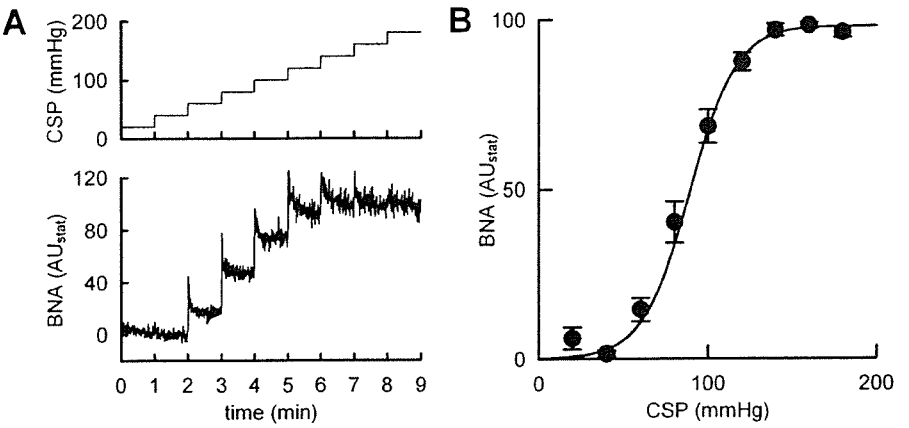

Fig. 2. A: Representative time series of carotid sinus pressure (CSP) and afferent baroreceptor nerve activity (BNA) during the stepwise input protocol. CSP and BNA were resampled at 2 Hz for the panels. CSP was increased from 20 to 180 mmHg every minute with a pressure step of 20 mmHg. **B: The CSP-BNA relationship averaged from all animals.** The CSP-BNA relationship revealed sigmoidal nonlinearity. The closed circles represent mean values, and the error bars indicate mean ± SEM values at each CSP. The solid curve indicates the logistic function derived from averaged parameters shown in Table 1. AU_{stat}: arbitrary units for static analysis.

very small up to 3 Hz. The phase delay between CSP and actual pressure should be taken into account in the interpretation of phase data of the transfer function from CSP to BNA shown in Fig. 1C. The phase delay between CSP and BNA noted in the frequency range above 1 Hz would be chiefly attributable to the phase delay between CSP and the actual pressure imposed on the carotid sinus area.

Derivative characteristics of the baroreflex neural arc contribute to the optimization of the AP regulation by the carotid sinus baroreflex [1]. Although Franz *et al.* [6] reported dynamic characteristics of single baroreceptor fiber activity in the rabbit carotid sinus in the frequency range from 0.078 to 2.5 Hz by using sinusoidal inputs, the derivative characteristics were obscure in that frequency range. As shown in Fig. 1C, dynamic gain from CSP to BNA augmented to approximately 1.7 with increasing frequency from 0.01 to 0.5 Hz, indicating the existence of the derivative characteristics. When the transfer function from CSP input to efferent SNA was identified in our previous study [15], dynamic gain increased to 3.8-fold for cardiac SNA and to 2.3-fold for renal SNA, with increasing frequency from 0.01 to 0.5 Hz (see Fig. 3 in Ref. 15). Thus approximately 40% (for cardiac) and 64% (for renal) of the derivative characteristic may be explained by the dynamic characteristics of the CSP-BNA transduction.

High-cut characteristics of the baroreflex neural arc attenuate high-frequency components in the input pressure and preserve the baroreflex gain against pulsatile pressure [4]. As shown in Fig. 1C, the dynamic gain of the transfer function from CSP to BNA was relatively constant in the frequency range from 0.3 to 3 Hz and showed no high-cut characteristics. Therefore the high-cut characteristics of the baroreflex neural arc are primarily attributable to the central processing from BNA to efferent SNA. In other words, the dynamic characteristics from BNA to efferent SNA should reveal high-cut characteristics with a corner frequency of approximately 0.8 Hz. The mechanism for the putative high-cut characteristics in the central processing remains unclear. The frequency-dependent depression of the signal transduction in the nucleus tractus solitarii (NTS) neurons [16] may be related to the upper frequency limit of central processing. However, the frequency-dependent depression refers to the phenomenon related to the stimulation frequency itself, whereas the high-cut characteristics refer to the attenuation of the system response related to the modulation frequency of the input. Further information is required to reconcile the putative high-cut characteristics and the frequency-dependent depression in the baroreflex central pathway.

The dynamic characteristics of the carotid sinus baroreceptor transduction were generally similar to those of the baroreceptor transduction of the aortic depressor nerve in rabbits [11]. However, a slight difference can be noted as follows. The gain increase from 0.01 to 0.1 Hz was approximately 1.7-fold (4.6 dB/decade) for the carotid sinus baroreceptors (Fig. 1C), whereas it was approximately 2-fold (6.0 dB/decade) for the aortic baroreceptors (see Fig. 5 in Ref. 11). In the rat aortic baroreceptor preparation, Brown *et al.* [5] demonstrated that myelinated fibers showed peaking in the frequency response, whereas unmyelinated fibers did not. The myelinated and unmyelinated fiber composition would affect the dynamic characteristics of multifiber BNA. Brown *et al.* [5] also demonstrated that the peaking of myelinated fiber response reached approximately 4 dB/decade in normotensive rats and approximately 6 dB/decade in spontaneously hyperten-

sive rats. Therefore the difference between the carotid sinus and aortic baroreceptor transductions, though it seems subtle, may reflect the difference in the myelinated and unmyelinated fiber composition and/or the difference in the prevailing pressure between the carotid sinus and aortic baroreceptors.

Static characteristics of the carotid sinus baroreceptor transduction. The static characteristics of the CSP-BNA transduction showed sigmoidal nonlinearity (Fig. 2B). BNA increased with CSP in the pressure range from 40 to 160 mmHg. In the single fiber preparation of the rabbit carotid sinus baroreceptors, the stimulus-response curve is fairly linear in each fiber between threshold pressure and saturation pressure [6]. However, the threshold pressure and the slope of the linear range vary considerably among fibers. Such variations in the static characteristics of single baroreceptor fiber activities are lumped together, possibly forming the sigmoidal relationship between CSP and multifiber BNA. The slope coefficient of the CSP-BNA relationship (Table 1) was smaller than the slope coefficient of the CSP-SNA relationship (0.10–0.12) determined in our previous studies [15, 17, 18]. In other words, the operating range of the system, which is inversely related to the slope coefficient [14], was wider for the CSP-BNA relationship than for the CSP-SNA relationship. The finding is consistent with our speculation, which is based on input-size and operating-point dependence of the baroreflex neural arc transfer function, that the static CSP-BNA relationship alone does not determine the overall nonlinearity of the neural arc characteristics [2, 3].

The midpoint pressure of the CSP-BNA relationship was approximately 90 mmHg, which is lower than the midpoint pressure of the CSP-SNA relationship (100–110 mmHg) determined in our previous studies [15, 17, 18]. The possibility cannot be ruled out, however, that the extensive surgical operation necessary for the BNA recording had altered the mechanical properties of the carotid sinus area differently from the preparation for the carotid sinus isolation alone. Although we had intended to simultaneously record afferent BNA and efferent SNA, the SNA and AP did not respond to the CSP input in the present experimental settings. A large portion of the baroreceptor afferent fibers may have been damaged because of fragility during the preparation. The difficulty results because we could not know, based on the magnitude of BNA, what percent of the nerve fibers were really kept intact. Further efforts are required to directly demonstrate the difference in the static input-output characteristics between the CSP-BNA relationship and the CSP-SNA relationship.

In conclusion, although a slight difference was noted, the dynamic characteristics of the carotid sinus baroreceptor transduction were similar to those of the aortic baroreceptor transduction in rabbits. The CSP-BNA transduction partly explained the derivative characteristics, but not the high-cut characteristics found in the neural arc transfer function from CSP to efferent SNA. The present results suggest the importance of the central processing from BNA to efferent SNA to account for the overall dynamic characteristics of the baroreflex neural arc.

This study was supported by the Health and Labour Sciences Research Grant for Research on Advanced Medical Technology from the Ministry of Health Labour and Welfare of Japan (H14-Nano-002), and by the Program for Promotion of Fundamental Studies in Health Science of the Pharmaceuticals and Medical Devices Agency of Japan.

REFERENCES

1. Ikeda Y, Kawada T, Sugimachi M, Kawaguchi O, Shishido T, Sato T, Miyano H, Matsuura W, Alexander J Jr, and Sunagawa K: Neural arc of baroreflex optimizes dynamic pressure regulation in achieving both stability and quickness. Am J Physiol Heart Circ Physiol 271: H882–H890, 1996
2. Kawada T, Uemura K, Kashihara K, Kamiya A, Sugimachi M, and Sunagawa K: A derivative-sigmoidal model reproduces operating point-dependent baroreflex neural arc transfer characteristics. Am J Physiol Heart Circ Physiol 286: H2272–H2279, 2004
3. Kawada T, Yanagiya Y, Uemura K, Miyamoto T, Zheng C, Li M, Sugimachi M, and Sunagawa K: Input-size dependence of the baroreflex neural arc transfer characteristics. Am J Physiol Heart Circ Physiol 284: H404–H415, 2003
4. Kawada T, Zheng C, Yanagiya Y, Uemura K, Miyamoto T, Inagaki M, Shishido T, Sugimachi M, and Sunagawa K: High-cut characteristics of the baroreflex neural arc preserve baroreflex gain against pulsatile pressure. Am J Physiol Heart Circ Physiol 282: H1149–H1156, 2002
5. Brown AM, Saum W, and Yasui S: Baroreceptor dynamics and their relationship to afferent fiber type and hypertension. Circ Res 42: 694–702, 1978
6. Franz GN, Sher AM, and Ito CS: Small signal characteristics of carotid sinus baroreceptors of rabbits. J Appl Physiol 30: 527–535, 1971
7. Spickler JW and Kezdi P: Dynamic response characteristics of carotid sinus baroreceptors. Am J Physiol 212: 472–476, 1967
8. Marmarelis PZ and Marmarelis VZ: Analysis of Physiological Systems, Plenum, New York, pp 131–221, 1978
9. Kawada T, Fujiki N, and Hosomi H: Systems analysis of the carotid sinus baroreflex system using a sum-of-sinusoidal input. Jpn J Physiol 42: 15–34, 1992
10. Sugimachi M, Imaizumi T, Sunagawa K, Hirooka Y, Todaka K, Takeshita A, and Nakamura M: A new method

to identify dynamic transduction properties of aortic baroreceptors. Am J Physiol Heart Circ Physiol 258: H887–H895, 1990
11. Sato T, Kawada T, Shishido T, Miyano H, Inagaki M, Miyashita H, Sugimachi M, Knuepfer MM, and Sunagawa K: Dynamic transduction properties of in situ baroreceptors of rabbits aortic depressor nerve. Am J Physiol Heart Circ Physiol 274: H358–H365, 1998
12. Pelletier CL, Clement DL, and Shepherd JT: Comparison of afferent activity of canine aortic and sinus nerves. Circ Res 31: 557–568, 1972
13. Bendat J and Piersol A: Random Data 3rd Ed. John Wiley & Sons, New York, pp 189–271, 2000
14. Kent BB, Drane JW, Blumenstein B, and Manning JW: A mathematical model to assess changes in the baroreceptor reflex. Cardiology 57: 295–310, 1972
15. Kawada T, Shishido T, Inagaki M, Tatewaki T, Zheng C, Yanagiya Y, Sugimachi M, and Sunagawa K: Differential dynamic baroreflex regulation of cardiac and renal sympathetic nerve activities. Am J Physiol Heart Circ Physiol 280: H1581–H1590, 2001
16. Liu Z, Chen C, and Bonham AC: Frequency limits on aortic baroreceptor input to nucleus tractus solitarii. Am J Physiol Heart Circ Physiol 278: H577–H585, 2000
17. Kawada T, Uemura K, Kashihara K, Jin Y, Li M, Zheng C, Sugimachi M, and Sunagawa K: Uniformity in dynamic baroreflex regulation of left and right cardiac sympathetic nerve activities. Am J Physiol Regul Integr Comp Physiol 284: R1506–R1512, 2003
18. Yamamoto K, Kawada T, Kamiya A, Takaki H, Miyamoto T, Sugimachi M, and Sunagawa K: Muscle mechanoreflex induces the pressor response by resetting the arterial baroreflex neural arc. Am J Physiol Heart Circ Physiol 286: H1382–H1388, 2004

Acta Physiol Scand 2005, 184, 187–193

Myocardial interstitial choline and glutamate levels during acute myocardial ischaemia and local ouabain administration

T. Kawada,[1] T. Yamazaki,[2] T. Akiyama,[2] T. Shishido,[1] H. Mori[2] and M. Sugimachi[1]

1 *Department of Cardiovascular Dynamics, National Cardiovascular Center Research Institute, Osaka, Japan*

2 *Department of Cardiac Physiology, National Cardiovascular Center Research Institute, Osaka, Japan*

Received 25 November 2004, accepted 16 March 2005
Correspondence: T. Kawada, Department of Cardiovascular Dynamics, National Cardiovascular Center Research Institute, 5-7-1 Fujishirodai, Suita, Osaka 565-8565, Japan.
E-mail: torukawa@res.ncvc.go.jp

Abstract

Aim: Noradrenaline (NA) uptake transporters are known to reverse their action during acute myocardial ischaemia and to contribute to ischaemia-induced myocardial interstitial NA release. By contrast, functional roles of choline and glutamate transporters during acute myocardial ischaemia remain to be investigated. Because both transporters are driven by the normal Na^+ gradient across the plasma membrane in a similar manner to NA transporters, the loss of Na^+ gradient would affect the transporter function, which would in turn alter myocardial interstitial choline and glutamate levels. The aim of the present study was to examine the effects of acute myocardial ischaemia and the inhibition of Na^+,K^+-ATPase on myocardial interstitial glutamate and choline levels.

Methods: In anaesthetized cats, we measured myocardial interstitial glutamate and choline levels while inducing acute myocardial ischaemia or inhibiting Na^+,K^+-ATPase by local administration of ouabain.

Results: The choline level was not changed significantly by ischaemia (from 0.93 ± 0.06 to 0.82 ± 0.13 μM, mean ± SE, $n = 6$) and was decreased slightly by ouabain (from 1.30 ± 0.06 to 1.05 ± 0.07 μM, $P < 0.05$, $n = 6$). The glutamate level was significantly increased from 9.5 ± 1.9 to 34.7 ± 6.1 μM by ischaemia ($P < 0.01$, $n = 6$) and from 8.9 ± 1.0 to 15.9 ± 2.3 μM by ouabain ($P < 0.05$, $n = 6$). Inhibition of glutamate transport by *trans*-L-pyrrolidine-2,4-dicarboxylate (*t*-PDC) suppressed ischaemia- and ouabain-induced glutamate release.

Conclusion: Myocardial interstitial choline level was not increased by acute myocardial ischaemia or by Na^+,K^+-ATPase inhibition. By contrast, myocardial interstitial glutamate level was increased by both interventions. The glutamate transporter contributed to glutamate release via retrograde transport.

Keywords acetylcholine, cardiac microdialysis, cats, coronary artery occlusion, myocardium, noradrenaline.

Acute myocardial ischaemia causes oxygen depletion and loss of ATP in the ischaemic region (Hearse 1979). Blockade of H^+-ATPase leads to noradrenaline (NA) leakage from storage vesicles and axoplasmic NA accumulation (Schömig *et al.* 1988). Intracellular acidosis causes Na^+ influx via Na^+/H^+ exchange. Inhibition of Na^+,K^+-ATPase activity reduces the Na^+ gradient across the plasma membrane. Because NA uptake transporters are driven by the normal Na^+ electrochemical gradient across the plasma membrane,

axoplasmic NA accumulation and reduction of the Na^+ gradient cause reverse transport of NA from the intracellular space to the extracellular space (Schwartz 2000). Acute myocardial ischaemia evokes the myocardial interstitial NA release in the ischaemic region via retrograde NA transport, independently of efferent sympathetic nerve activity (Schömig *et al.* 1984, Yamazaki *et al.* 1996, Akiyama & Yamazaki 1999, Kawada *et al.* 2001a).

Similar to NA, choline and glutamate are taken up into cells by plasma membrane transporters driven by the Na^+ gradient (Schwartz 2000). We hypothesized that the loss of Na^+ gradient under ischaemic conditions would interfere with the transporter function, which would in turn alter myocardial interstitial choline and glutamate levels. Choline release has been suggested as an index of ischaemic degradation of the myocardial phospholipid bilayer in isolated, Tyrode solution-perfused rat hearts (Brühl *et al.* 2004). Glutamate can be a preferred myocardial fuel during ischaemia and may have protective effects on ischaemic myocardium (Arsenian 1998). Measuring myocardial interstitial levels of these molecules *in vivo* would contribute to understanding the pathophysiology of acute myocardial ischaemia. To test the hypothesis, we employed an *in vivo* cardiac microdialysis technique and measured myocardial interstitial choline and glutamate levels in anaesthetized cats (Akiyama *et al.* 1991, 1994, Yamazaki *et al.* 1997, Kawada *et al.* 2001b). Acute myocardial ischaemia inevitably affects systemic haemodynamics and perfusion of the heart. To minimize such haemodynamic effects, we also examined the effects of Na^+,K^+-ATPase inhibition on the myocardial interstitial choline and glutamate levels by locally administering ouabain through a dialysis probe (Yamazaki *et al.* 1999, Kawada *et al.* 2002). The results of the present study indicated that the myocardial interstitial choline level was not increased by acute myocardial ischaemia or by Na^+,K^+-ATPase inhibition. By contrast, the myocardial interstitial glutamate level was increased by both interventions. The glutamate transporter contributed to glutamate release via retrograde transport.

Materials and methods

Surgical preparation

Animal care was conducted in strict accordance with the *Guiding Principles for the Care and Use of Animals in the Field of Physiological Sciences* approved by the Physiological Society of Japan. Adult cats weighing 2.0–4.8 kg were anaesthetized via an intraperitoneal injection of pentobarbital sodium (30–35 mg kg^{-1}) and ventilated mechanically with room air mixed with oxygen. The depth of anaesthesia was maintained with a continuous intravenous infusion of pentobarbital sodium (1–2 mg kg^{-1} h^{-1}) through a catheter inserted via the right femoral vein. Mean systemic arterial pressure was monitored from a catheter inserted via the right femoral artery.

With the animal in the lateral position, the left fifth and sixth ribs were resected to expose the heart. When a coronary occlusion was necessary, a 3-0 silk suture was prepared around the left anterior descending coronary artery (LAD) just distal to the first diagonal branch. With a fine guiding needle, a dialysis probe was implanted into the left ventricular free wall perfused by the LAD. Heparin sodium (100 U kg^{-1} bolus injection followed by a maintenance dose of 50 U kg^{-1} h^{-1}) was administered intravenously to prevent blood coagulation. At the end of the experiment the experimental animals were killed by an overdose of pentobarbital sodium. We confirmed that the dialysis probe had been implanted within the left ventricular myocardium.

Dialysis technique

We designed a transverse dialysis probe (Akiyama *et al.* 1991, 1994). For measurements of small molecular compounds including ACh, choline, and glutamate, we used a dialysis fibre of 50 000 molecular weight cutoff (13 mm length, 310 μm OD, 200 μm ID; PAN-1200, Asahi Chemical, Osaka, Japan) with both ends glued to polyethylene tubes (20 cm length, 500 μm OD, 200 μm ID). The dialysis probe was perfused at a rate of 2 μL min^{-1} with Ringer solution. Each sample was collected in a microtube containing 3 μL of phosphate buffer (100 mM, pH 3.5). A cholinesterase inhibitor eserine (100 μM) was added to the perfusate to measure ACh. A preliminary examination indicated that whether the perfusate-contained eserine did not affect myocardial interstitial choline levels significantly. Dead space volume between the dialysis fibre and the sample microtube was identical for ACh, choline, and glutamate measurements, and the sampling was performed taking into account the time for dialysate to traverse the dead space volume.

The dialysate ACh and choline levels were measured directly by high-performance liquid chromatography with electrochemical detection. The absolute detection limits of ACh and choline, determined with a signal-to-noise ratio of 3, were 10 and 5 fmol per injection, respectively. The dialysate glutamate level was measured by kinetic enzymatic analysis with CMA 600. The absolute detection limit of glutamate was 1 μM per injection.

Protocols

All protocols were started from 2 h after implanting the dialysis probe. To examine changes in myocardial

interstitial ACh and choline levels during acute myocardial ischaemia ($n = 6$), after collecting a 15-min baseline dialysate sample, we occluded the LAD for 60 min and obtained four consecutive 15-min dialysate samples. The full-length of the implanted dialysis fibre was located within the ischaemic area judged by discoloration of myocardium during the LAD occlusion. We then released the occlusion and collected a 15-min dialysate sample during reperfusion. To examine changes in myocardial ACh and choline levels in response to local ouabain administration ($n = 6$), after collecting a 15-min baseline dialysate sample, we replaced the perfusate with Ringer solution containing 100 μM ouabain and collected four consecutive 15-min dialysate samples.

In different groups of animals, myocardial interstitial glutamate levels were measured during acute myocardial ischaemia ($n = 6$) and during local administration of ouabain ($n = 6$). To elucidate the role of the glutamate transporter, we also examined the effects of glutamate transport inhibition by *trans*-L-pyrrolidine-2,4-dicarboxylate (*t*-PDC, 10 mM) on myocardial interstitial glutamate levels during acute myocardial ischaemia ($n = 7$) and local administration of ouabain ($n = 7$). *t*-PDC was locally administered through the dialysis probe to avoid systemic effects.

Statistical analysis

All data are presented as mean ± SE values. In each protocol, the effects of myocardial ischaemia or local ouabain administration were examined using one-way analysis of variance followed by Dunnett's test against the corresponding baseline level (Glantz 2002). The baseline as well as maximum glutamate levels with and without glutamate transport inhibition were compared by an unpaired *t*-test during acute myocardial ischaemia or during local ouabain administration (Glantz 2002). Differences were considered to be significant when $P < 0.05$.

Results

Figure 1a shows myocardial interstitial ACh level during acute myocardial ischaemia. The ACh level was increased by LAD occlusion, becoming approximately 15 times higher than the baseline level at 30–45 and 45–60 min of ischaemia. The ACh level decreased towards the baseline level upon reperfusion. Figure 1b illustrates myocardial interstitial choline level during acute myocardial ischaemia. The choline level did not change significantly throughout the ischaemic and reperfusion periods.

Figure 2a shows changes in myocardial interstitial ACh level during local administration of ouabain. The ACh level was increased by the inhibition of

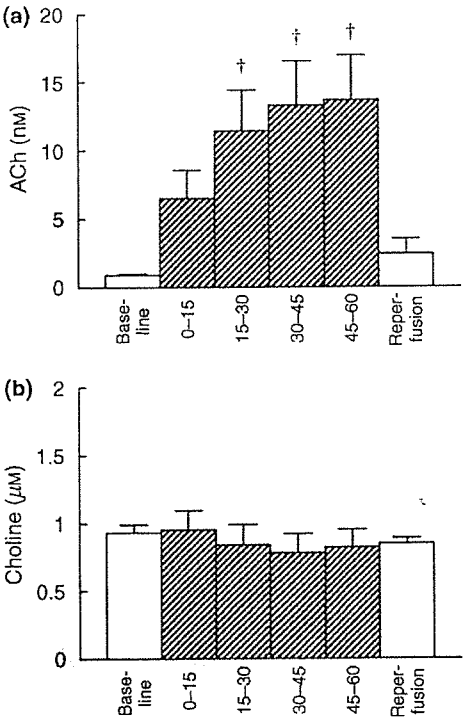

Figure 1 Changes in myocardial interstitial acetylcholine (ACh) level (a) and choline level (b) during coronary artery occlusion and reperfusion. Myocardial interstitial ACh level was significantly increased by acute myocardial ischaemia, while myocardial interstitial choline level was not changed. Data are mean ± SE. †$P < 0.01$ from baseline.

Na^+,K^+-ATPase, becoming approximately nine times higher than the baseline level at 15–30 min. The ACh level then decreased but remained significantly higher than the baseline level. Figure 2b illustrates the myocardial interstitial choline level during local administration of ouabain. The choline level was significantly lower at 0–15 and 45–60 min when compared with the baseline level.

Figure 3a shows changes in myocardial interstitial glutamate level during acute myocardial ischaemia. LAD occlusion increased the glutamate level to approximately 3.5 times higher than the baseline level at 0–15 min. Thereafter, the glutamate level was significantly higher than the baseline level throughout the ischaemic and reperfusion periods. Figure 3b illustrates the effects of glutamate transport inhibition on the ischaemia-induced glutamate release. The baseline glutamate level was significantly decreased by glutamate transport inhibition ($P < 0.05$). Although acute myocardial ischaemia and reperfusion significantly increased the glutamate level relative to the baseline level, the maximum glutamate level was attenuated to approximately one-fifth compared with that observed without glutamate transport inhibition ($P < 0.05$).